AGU PUBLICATIONS

JGR

Journal of Geophysical Research: Solid Earth

RESEARCH ARTICLE
10.1002/2014JB011327

Key Points:
- We image the crustal structure of the Taiwan mountain belt
- Low seismic velocities in the middle crust suggest thickening of Eurasian crust
- The Luzon Arc and Forearc block are strongly deformed in eastern Taiwan

Correspondence to:
H. J. A. Van Avendonk,
harm@ig.utexas.edu

Citation:
Van Avendonk, H. J. A., H. Kuo-Chen, K. D. McIntosh, L. L. Lavier, D. A. Okaya, F. T. Wu, C. Y. Wang, C. S. Lee, and C. S. Liu (2014), Deep crustal structure of an arc-continent collision: Constraints from seismic traveltimes in central Taiwan and the Philippine Sea, *J. Geophys. Res. Solid Earth*, *119*, doi:10.1002/2014JB011327.

Received 27 MAY 2014
Accepted 21 OCT 2014
Accepted article online 27 OCT 2014

Deep crustal structure of an arc-continent collision: Constraints from seismic traveltimes in central Taiwan and the Philippine Sea

H. J. A. Van Avendonk[1], H. Kuo-Chen[2], K. D. McIntosh[1], L. L. Lavier[1], D. A. Okaya[3], F. T. Wu[3,4], C. Y. Wang[2], C. S. Lee[5], and C. S. Liu[6]

[1]Institute for Geophysics, Jackson School of Geosciences, University of Texas at Austin, Austin, Texas, USA, [2]Institute of Geophysics, National Central University, Jhongli, Taiwan, [3]Department of Earth Sciences, University of Southern California, Los Angeles, California, USA, [4]Department of Geological and Environmental Sciences, State University of New York at Binghamton, Binghamton, New York, USA, [5]Department of Geophysics, National Taiwan Ocean University, Keelung, Taiwan, [6]Institute of Oceanography, National Taiwan University, Taipei, Taiwan

Abstract The collision of continental crust of the Eurasian Plate with the overriding Luzon Arc in central Taiwan has led to compression, uplift, and exhumation of rocks that were originally part of the Chinese rifted margin. Though the kinematics of the fold-thrust belt on the west side of the orogen has been described in detail, the style of deformation in the lower crust beneath Taiwan is still not well understood. In addition, the fate of the Luzon Arc and Forearc in the collision is also not clear. Compressional wave arrival times from active-source and earthquake seismic data from the Taiwan Integrated Geodynamic Research program constrain the seismic velocity structure of the lithosphere along transect T5, an east-west corridor in central Taiwan. The results of our analysis indicate that the continental crust of the Eurasian margin forms a broad crustal root beneath central Taiwan, possibly with a thickness of 55 km. Compressional seismic velocities beneath the Central Range of Taiwan are as low as 5.5 km/s at 25 km depth, whereas *P* wave seismic velocities in the middle crust on the eastern flank of the Taiwan mountain belt average 6.5–7.0 km/s. This suggests that the incoming sediments and upper crust of the Eurasian Plate are buried to midcrustal depth in the western flank of the orogen before they are exhumed in the Central Range. To the east, the Luzon Arc and Forearc are deformed beneath the Coastal Range of central Taiwan. Fragments of the rifted margin of the South China Sea that were accreted in the early stages of the collision form a new backstop that controls the exhumation of Eurasian strata to the west in this evolving mountain belt.

1. Introduction

Among earth scientists there is a consensus that the accretion of island arc terranes to continental margins has contributed to the rejuvenation and growth of the Earth's continental crust over the Phanerozoic [*McLennan and Taylor*, 1982; *Sengör et al.*, 1993; *Holbrook et al.*, 1999; *DeBari and Greene*, 2011], even if the process of arc-continent collision is not fully understood. Arc crust is often more mafic in its mean composition than the global average continental crust [*Shillington et al.*, 2004; *Tatsumi et al.*, 2008], but over the time that subduction zones are active, island arc crusts may evolve to a more andesitic composition by differentiation and delamination of dense lower crust [*Jull and Kelemen*, 2001; *Jagoutz and Behn*, 2013]. In addition, arc-continent collision may generally preserve relatively silicic arc crustal terranes in mountain belts, whereas more mafic components may be returned to the mantle [*Draut and Clift*, 2013]. Along the marginal basins of Southeast Asia, where arc-continent collision is in progress, volcanic arc rocks appear to make up a much smaller fraction of the new crust than the ubiquitous trench deposits [*Hall*, 2009]. The role of the island arc accretion may nonetheless be very important if arc fragments comprise a larger portion of the lower crust of the orogen or if they control the style of deformation as a backstop to the terrigenous sediments of the incoming plate. To understand the role of arc crustal blocks in the evolution of mountain belts along convergent margins, it is therefore important to image the deep-crustal structure of an active collision zone.

The island of Taiwan is widely considered one of the best locations on Earth to study arc accretion [*Byrne et al.*, 2011]. The closure of the northern South China Sea between the passive margin of China and the overriding Philippine Sea Plate has led to an arc-continent collision that formed the Taiwan mountain belt over a time span of approximately 6.5 Myr [*Huang et al.*, 1997; *Lin et al.*, 2003]. Due to the oblique convergence

between the Eurasian Plate and the Luzon Arc of the Philippine Sea Plate, this collision propagated from north to south in Taiwan [*Suppe*, 1984]. At present, rifted blocks of continental crust of the Chinese margin are entering the west facing accretionary prism adjacent to the Manila Trench south of Taiwan [*Eakin et al*., 2014]. The preexisting faulting architecture of the rifted margin facilitates the transfer of these crustal blocks to this growing wedge, forming the nucleus of the Taiwan mountain belt [*McIntosh et al*., 2013]. In central Taiwan the collision may have reached a steady state, where the influx of thick continental crust of the Eurasian Plate is balanced by rapid uplift and erosion of the orogenic wedge [*Stolar et al*., 2007]. In northern Taiwan, where the Luzon Arc volcanic edifice no longer forms a backstop, the orogen is now in a state of extensional collapse [*Teng*, 1996; *Clift et al*., 2008].

Perhaps the most studied aspect of the evolution of the Taiwan orogen is the development of a fold-thrust belt along its western flank [*Suppe*, 1981; *Mouthereau et al*., 2002; *Brown et al*., 2012]. Here the strata from the Chinese margin are deformed in thin, west vergent thrust sheets above a shear zone that dips eastward from the Taiwan Strait toward the mountain belt [*Simoes et al*., 2007]. If this décollement extends across Taiwan at just 5–10 km depth [*Carena et al*., 2002], the middle and lower crust of the Chinese margin could subduct without significant internal deformation. However, studies of seismicity and coseismic displacement [*Ching et al*., 2011; *Brown et al*., 2012; *Chuang et al*., 2013] show that thick sections of middle and lower crust of Taiwan are shortening as well. Whether contraction across the Taiwan mountain belt is accommodated largely by thin-skinned or thick-skinned deformation, ultimately gives us insight in the rheology of the two lithospheric plates that are involved in the collision. Given that the eastern margin of China was experiencing Andean-type subduction in the Late Cretaceous [*Lan et al*., 2008], followed by rifting in the Paleocene [*Lee and Lawver*, 1995], we would expect the Eurasian lithosphere to have a relatively young thermal age. It is therefore possible that the incoming Eurasian Plate is weak and that the crust of Taiwan is thickening by uniform shortening over a wide region [*Yamato et al*., 2009; *Mouthereau et al*., 2013]. On the other hand, the Taiwan orogen formed initially by accretion of strata and upper crustal rocks from the Chinese margin above an east dipping oceanic subduction zone [*McIntosh et al*., 2013], so eastward underthrusting of the Eurasian Plate [*Malavieille et al*., 2002], and underplating of its terrigenous strata [*Simoes et al*., 2007], may contribute to the growth of the crustal root of Taiwan as well.

To obtain new constraints on the mode of deformation during various stages of the collision, the 2008–2009 Taiwan Geodynamics Research (TAIGER) project produced several active-source seismic transects across the plate boundary in Taiwan [*McIntosh et al*., 2013] and in the Luzon Strait between the Philippines and Taiwan [*Lester et al*., 2013; *Eakin et al*., 2014]. In this paper we present an analysis of both active-source and earthquake seismic data to image the *P* wave seismic velocity structure along TAIGER transect T5 across the broadest section of the Taiwan mountain belt. We show that much of the Luzon Arc and Forearc, which forms a backstop for the orogen to the south, is deeply buried and deformed in the collision in central Taiwan.

2. Tectonic Setting

The island of Taiwan lies at the junction of the Manila Trench, where the oceanic lithosphere of the South China Sea subducts eastward beneath the Philippine Sea Plate, and the Ryukyu Trench, where the Philippine Sea Plate subducts northward beneath the Eurasian margin (Figure 1). Regional and global tomography images suggest that the Eurasian slab detaches at a depth of approximately 100 km beneath eastern and northern Taiwan, where the polarity of the subduction zone flips [*Lallemand et al*., 2001; *Huang et al*., 2014a]. Geodetic data show 80 mm/yr of northwest-southeast convergence between the Philippine Sea Plate and Eurasia at present [*Yu et al*., 1999]. In eastern Taiwan, approximately 30–40 mm/yr of this convergence is accommodated near the Longitudinal Valley Fault [*Yu and Kuo*, 2001], between the Coastal Range and Central Range. However, the differential motion between the Coastal Range and the Chinese margin decreases significantly in the northern portion of the Coastal Range [*Chang et al*., 2003], where the arc-continent collision has advanced farther than in the south.

West of the Longitudinal Valley, the major geologic units of Taiwan generally increase in metamorphic grade and the degree of deformation from west to east [*Ho*, 1986; *Beyssac et al*., 2007], which illustrates the asymmetry in the mode of contraction in the mountain belt [*Simoes et al*., 2007]. The coastal plain along Taiwan Strait overlies a foreland basin that developed due to the flexure of the Eurasian continental lithosphere adjacent to the young orogen [*Chou and Yu*, 2002; *Lin and Watts*, 2002; *Lester et al*., 2012]. In the

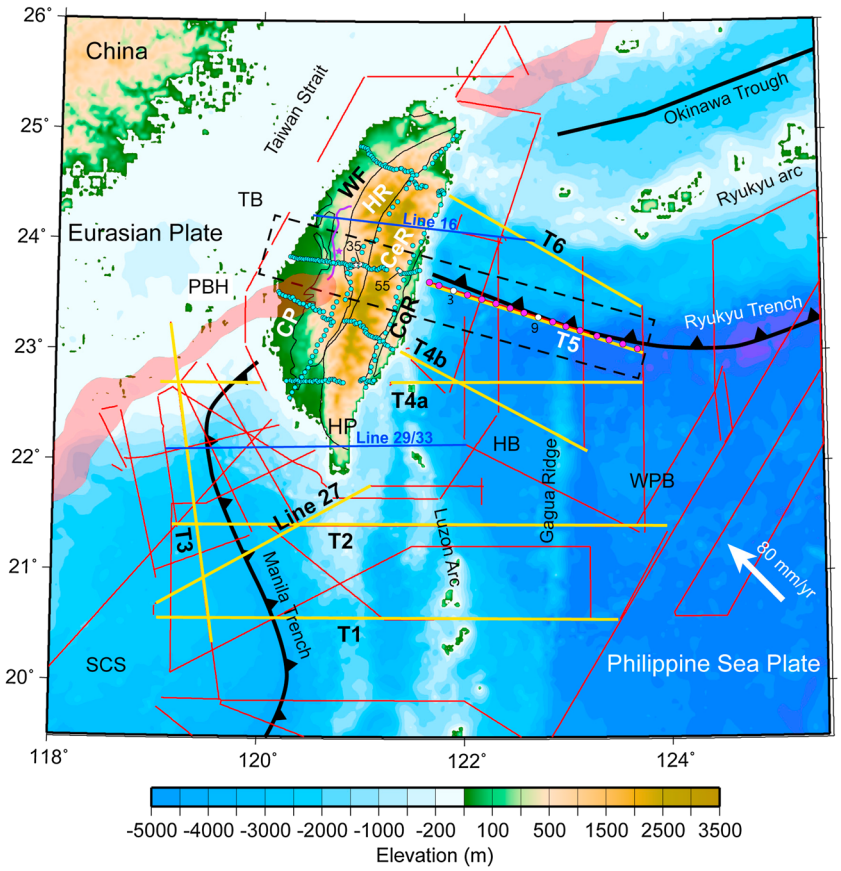

Figure 1. Overview map of the Taiwan region. The 2009 marine seismic TAIGER experiment included MCS lines (red), OBS lines (yellow, pink circles on transect T5), and onshore seismic stations (cyan circles). Taicrust lines 29/33 and 16 [*McIntosh et al.*, 2005] are in blue. CeR = Central Range; CP = Coastal Plain; CoR = Coastal Range; HB = Huatung Basin; HP = Hengchun Peninsula; HR = Hsüehshan Range; PBH = Peikang Basement High; SCS = South China Sea; TB = Taihsi Basin; WF = Western Foothills; WPB = West Philippine Basin. Purple line and star mark the Chelungpu Fault and the 1999 Chi-Chi earthquake. Red shading on the Chinese margin outlines the +80 nT Continental Margin Magnetic Anomaly (CMMA). The dashed box shows the location of Figure 9b.

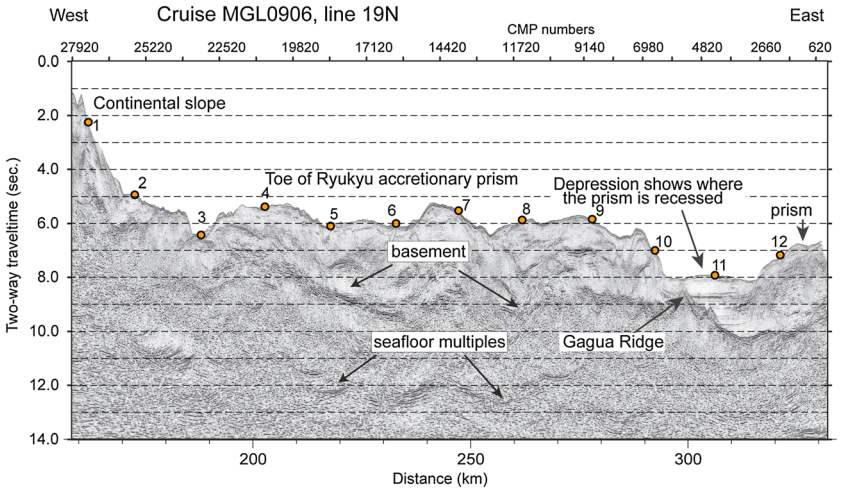

Figure 2. Time-migrated seismic reflection profile of line 19°N, which coincides with transect T5 east of Taiwan. The labeled orange circles indicate OBS locations on this transect.

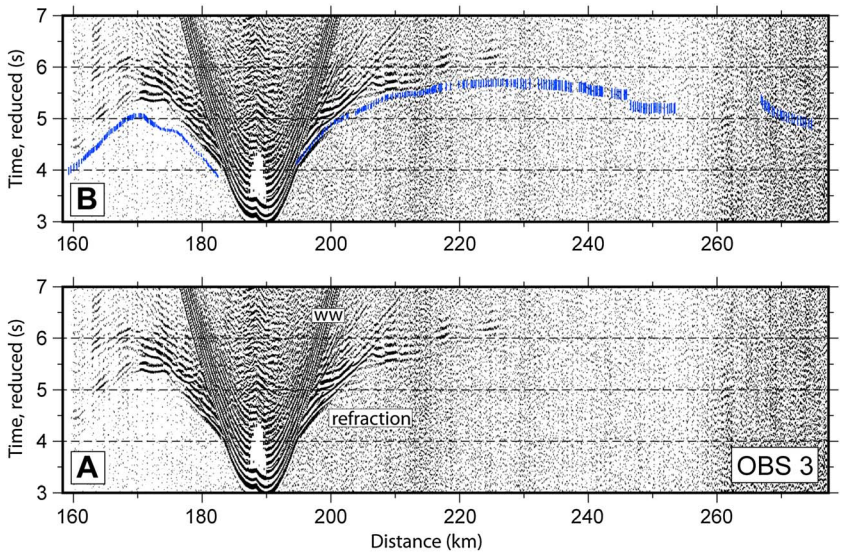

Figure 3. (a) Hydrophone record of the seismic refraction data from the marine seismic line T5 east of Taiwan, recorded by OBS 3 (Figure 1). The vertical axis is reduced by 7 km/s. ww = water wave. (b) The same panel as Figure 3a but with traveltime picks and uncertainties for the first-arriving refraction.

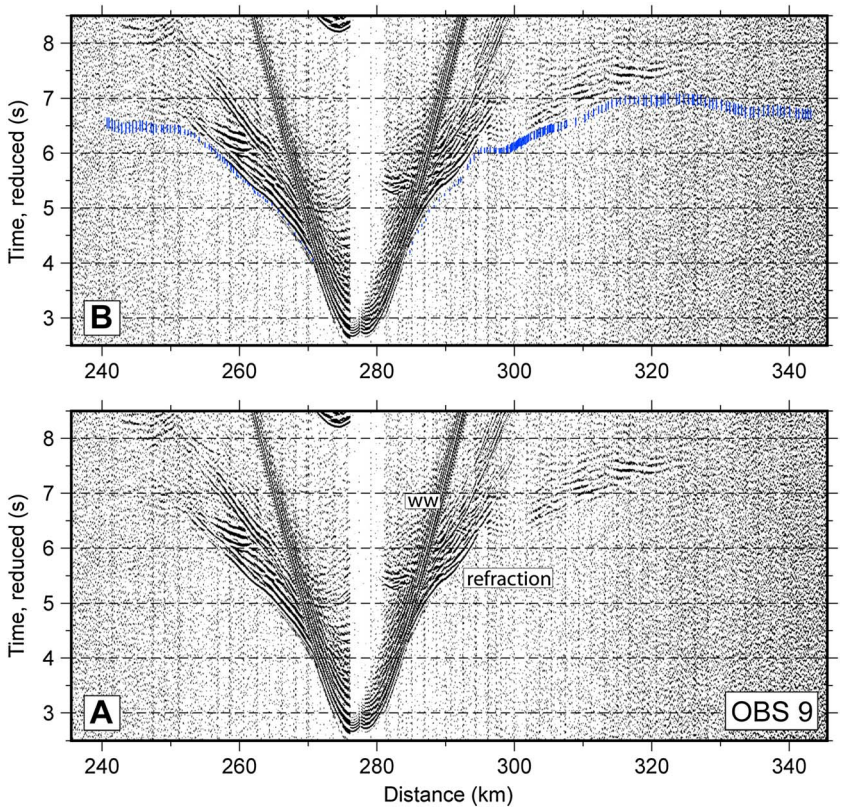

Figure 4. (a) Hydrophone record of the seismic refraction data from the marine seismic line T5 east of Taiwan, recorded by OBS 9 (Figure 1). The vertical axis is reduced by 7 km/s. (b) The same panel as Figure 4a but with traveltime picks and uncertainties for the first-arriving refraction.

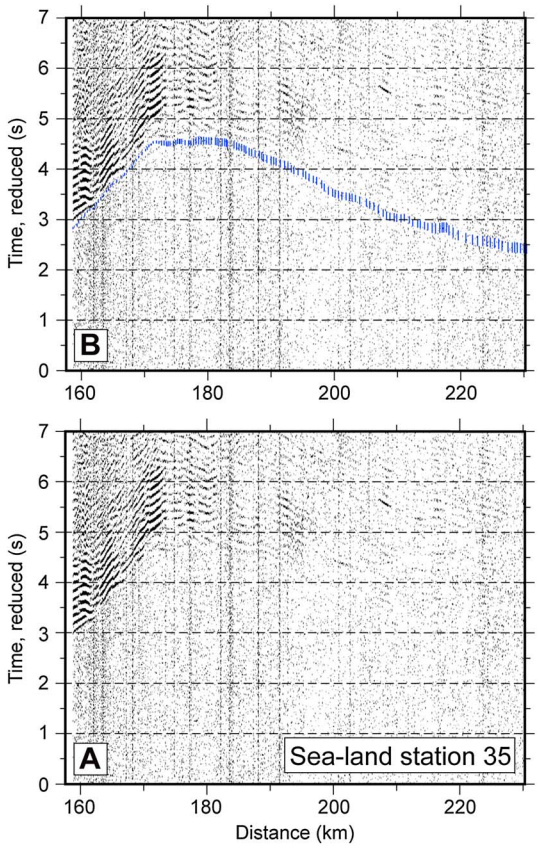

Figure 5. (a) Seismic refraction data from the marine seismic line T5 east of Taiwan, recorded onshore on T5 by station 35 at 89.6 km in this profile, in the Central Range (Figure 1). The vertical axis is reduced by 6 km/s. (b) The same panel as Figure 5a but with traveltime picks and uncertainties for the first-arriving refraction.

Western Foothills, strata of the foreland basin are deformed in the aforementioned west vergent fold-thrust belt [*Suppe*, 1981] along with pre-Neogene basement rocks of the Eurasian margin [*Mouthereau and Lacombe*, 2006]. The inversion of a rift basin on the Eurasian margin during recent (6.5 Ma) shortening has created the Hsüehshan Range in central and northern Taiwan [*Clark et al*., 1993; *Kidder et al*., 2012]. Farther east, the Central Range is composed of a slate belt that derives from sediments of the Chinese distal margin and the Tananao schist, continental basement that experienced greenschist metamorphism [*Teng*, 1990; *Lin*, 2002] mixed with sections of high-pressure metamorphosed oceanic rocks [*Ernst*, 1981; *Beyssac et al*., 2008].

Though the oblique convergence between the Philippine Sea Plate and Eurasian Plate is consistent with a southward propagation of the arc-continent collision [*Suppe*, 1984], it must be recognized that the geometry of the Chinese margin that entered the orogen from the west is not well known. In the Taiwan Strait, a large, positive magnetic anomaly lies parallel to the Chinese margin across the Peikang Basement High, where the thick crust of the Eurasian continent entered the collision [*Cheng*, 2004; *Byrne et al*., 2011] (Figure 1). This magnetic anomaly does not extend farther than central Taiwan, and a northwest striking line of high seismicity may reveal an ancient fracture zone and segment boundary of the Chinese margin [*Deffontaines et al*., 1997]. The lateral variation in crustal structure between the Peikang Basement High in the southwestern Taiwan Strait and the Taihsi Basin to the northwest (Figure 1) may have led to differences in the depth of thrusting and exhumation in the adjacent mountain belt [*Mouthereau and Petit*, 2003].

3. TAIGER Data

3.1. Data Acquisition

In 2008 and 2009, U.S. and Taiwanese scientists gathered seismic data on land and offshore along several transects in the Taiwan region [e.g., *Kuo-Chen et al*., 2012a, 2012b; *McIntosh et al*., 2013; *Eakin et al*., 2014] as part of the TAIGER project. Arrays of vertical-component seismographs from Incorporated Research Institutions for Seismology (IRIS)/PASSCAL (the Program for Array Seismic Studies of the Continental Lithosphere) deployed with 200 m spacing, recorded a test shot on transect T5. In addition, shots fired from the 6600 in^3 air gun array seismic vessel R/V *Marcus Langseth* at 150 m spacing were recorded both onshore and offshore on transect T5. The 2 Hz land seismometers were provided by PASSCAL, National Central University, and other Taiwanese universities. Ocean-bottom seismometers (OBSs) were contributed by National Taiwan Ocean University and the U.S. OBS Instrument Pool. These combined onshore and offshore seismic experiments were designed to obtain good coverage with wide-angle seismic data across the east coast of Taiwan. Since the land recorders on TAIGER transects recorded continuously for the duration of the marine seismic experiment, we were able to improve the data coverage of the deep crustal root by adding local earthquakes. To better image the basement morphology and sediment cover offshore, we also used the R/V *Marcus Langseth* to gather multichannel seismic (MCS) reflection data on its 6 km long streamer with 50 m shot spacing.

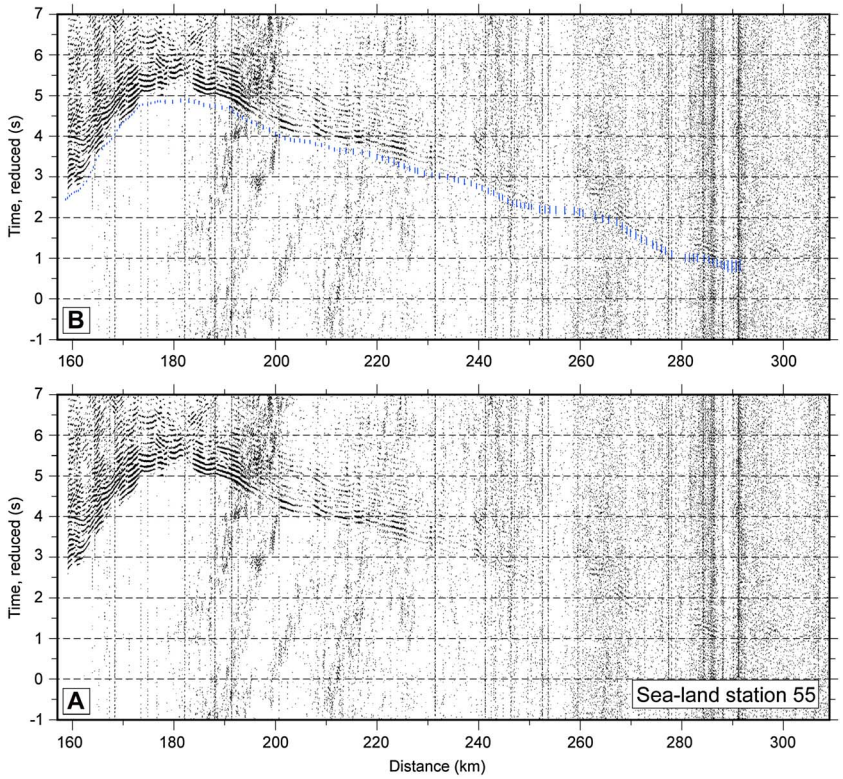

Figure 6. Seismic refraction data from the marine seismic line T5 east of Taiwan, recorded onshore on T5 by station 55 at 129.0 km in this profile, in the Coastal Range (Figure 1). The vertical axis is reduced by 6 km/s. (b) The same panel as Figure 6a but with traveltime picks and uncertainties for the first-arriving refraction.

3.2. Data Processing and Traveltime Picks

We produced a time-migrated seismic reflection image of the shallow structure of the section of transect T5 on the Philippine Sea Plate using the TAIGER MCS data (Figure 2). This marine seismic reflection line roughly follows the axis of the Ryukyu Trench, south of the Ryukyu Arc (Figure 1). Between 180 km and 300 km, the sediment cover imaged along this profile is part of the toe of the Ryukyu accretionary prism. The top of crystalline basement of the Philippine Sea Plate can be distinguished here 1.5 to 2.5 s two-way time beneath the seafloor. Farther east, the subducting Gagua Ridge has created a recess in the accretionary prism, such that the flat seafloor of the Huatung Basin adjacent to this bathymetric high intersects the seismic reflection profile. Though our seismic processing scheme included multiple attenuation [*Lester and McIntosh*, 2012], the Moho of the Philippine Sea Plate is obscured by multiples.

The seismic refraction data from the 16 OBSs along transect T5 on the Philippine Sea Plate show the direct wave in water, which we used to relocate instruments on the seafloor, as well as turning waves from the sediments and basement. After band-pass filtering of the data, we picked 2368 first-arriving traveltimes on all receiver gathers and visually assigned uncertainties that generally increase from 50 ms at source-receiver offsets smaller than 10 km, to 200 ms at offsets larger than 40 km on some instruments. The distance between traveltime picks along the shot line averaged 500 m. Two OBS data examples with traveltime picks are shown in Figures 3 and 4. Though OBS 3 (Figure 3) was positioned much closer to the Taiwan coast than OBS 4 (Figure 4), the data appear similar, which suggests that the crustal structure in the Huatung Basin is laterally quite homogeneous. We only picked first-arriving phases for our study, but a wide-angle Moho reflection can be seen on both receiver gathers at 30–40 km source-receiver offset.

The traveltime data set for TAIGER Transect T5 also includes 4554 picks from the onshore-offshore wide-angle data. In the Taiwan Strait, we used onshore records of one air gun shot from the R/V *Marcus Langseth* line parallel to the coast in the Taiwan Strait, where it crosses transect T5. Since we did not deploy a streamer or OBSs in the Taiwan Strait during the TAIGER program, this onshore-offshore record provides our only

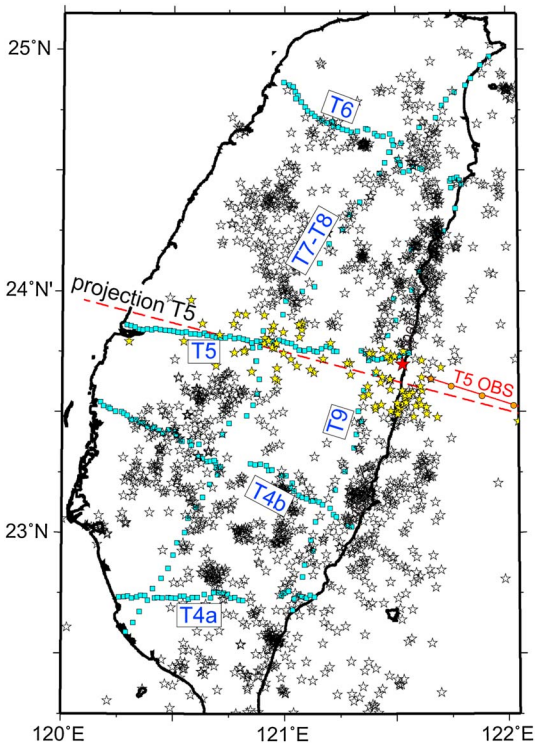

Figure 7. Map of linear arrays of three-component seismographs (cyan circles) along the TAIGER transects. The red solid line shows the marine shot line and OBSs (orange circles) offshore eastern Taiwan. The red dashed line represents the projection profile along which we carry out the 2-D tomographic inversion. White stars indicate the location of earthquakes of magnitude larger than 1.5 recorded by the TAIGER array. Yellow stars show the events used in this study of transect T5. The red star represents event 75, shown in Figure 8.

active-source seismic constraint on the deep structure of the foreland basin. In the Philippine Sea, we used onshore records from the MCS shot line along T5 perpendicular to the coast (Figure 1). On transect T5, a total of 61 Reftek stations recorded the air gun shots with a combination of L-22 (2 Hz) and L28 (4.5 Hz) sensors. After band-pass filtering, we picked first-arriving phases in the receiver gathers with an average spacing of 500 m, and uncertainties between 50 ms and 300 ms. The data from station 35 (Figure 5) and station 55 (Figure 6) illustrate the variability in data quality between these onshore-offshore records, which could be affected by environmental noise and differences in ground coupling. Though some of the records are of excellent quality, we cannot identify deeper phases, such as Moho reflections, with confidence.

During the TAIGER deployment, the dense array of three-component land seismometers recorded approximately 2000 earthquakes with a magnitude larger than 1.5 in and around Taiwan (Figure 7). Arrival times of a subset of these local earthquakes and teleseismic events were used by *Kuo-Chen et al.* [2012a, 2012b] to construct 3-D compressional and shear wave seismic velocity models. To improve our constraints on the 2-D structure along TAIGER line T5, we selected 84 of these local earthquakes with an epicenter within 15 km of the transect. We only used events that produced clear *P* and *S* wave arrivals on several of the TAIGER linear onshore-offshore instrument arrays. With these arrival times, we relocated the events in the 3-D *P* and *S* wave models of *Kuo-Chen et al.* [2012a, 2012b]. Traveltime pick uncertainties of the earthquake arrivals vary from 100 ms to 350 ms, which is larger than the uncertainties of most active-source seismic picks. However, the 3350 *P* wave traveltimes from these 84 events are critically important for imaging the deep crustal structure along this transect T5, since they illuminate the structure of the crustal root from all depths, up to 65 km. Figure 8 shows the record of a magnitude 3.4 earthquake at the east coast near transect T5. The *P* and *S* wave arrivals from all transects help to constrain the origin time and location. Subsequently, we use the *P* wave arrivals from stations along T5 to help constrain the compressional seismic velocity structure.

4. Traveltime Tomography

After assembling the traveltime table for first-arriving compressional waves from source-receiver pairs in the vicinity of transect T5, we traced raypaths between all sources and receivers in with the shortest path method [*Moser*, 1991] and ray bending [*Moser et al.*, 1992; *Van Avendonk et al.*, 2001]. The air gun shots in the Philippine Sea and the OBSs are positioned approximately along a straight line (Figure 1), so we calculated the corresponding raypaths and traveltimes along a 2-D profile. On the other hand, to obtain accurate traveltime calculations for the earthquake and onshore-offshore data, we applied 3-D ray tracing [*Van Avendonk et al.*, 2001, 2004b], since most sources and receivers are located at least several kilometers from the great circle arc through T5.

After we chose a simple starting model based on the earlier work of *McIntosh et al.* [2005] and *Kuo-Chen et al.* [2012a], we iterated between ray tracing and 2-D regularized inversions for seismic velocity structure in a

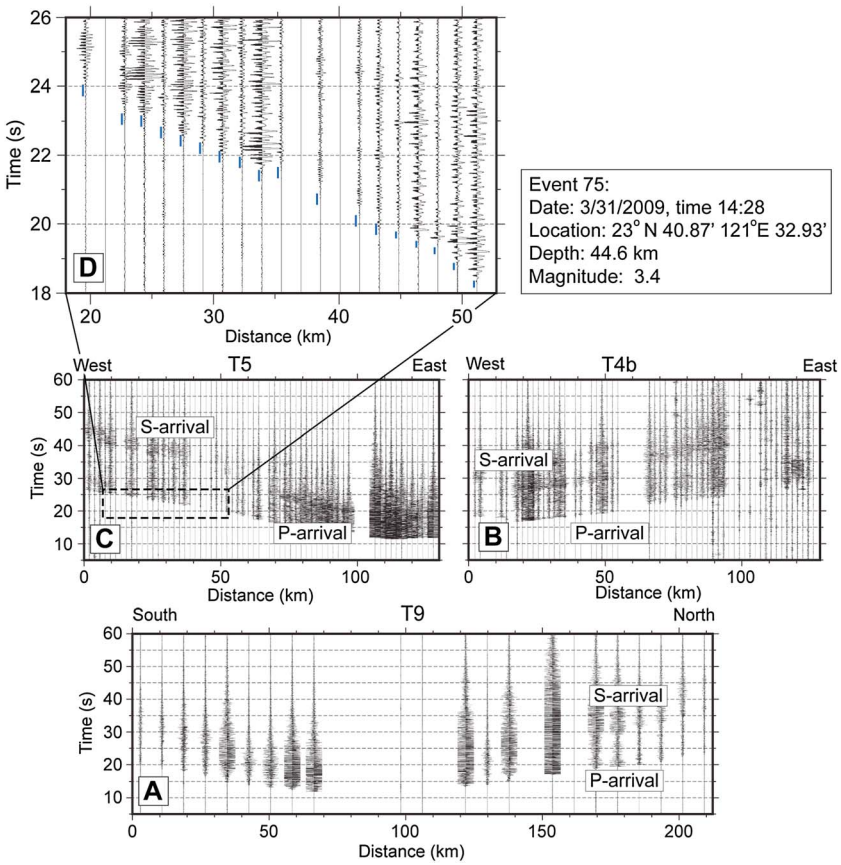

Figure 8. Data from an earthquake 75, off the east coast of Taiwan, recorded by land seismographs on (a) T9, (b) T4b, and (c) T5. *P* and *S* wave traveltimes are used for relocating this event. (d) A detail of the data from T5 with picked traveltimes and uncertainties (in blue).

vertical plane through transect T5 [*Van Avendonk et al*., 2004b]. In the inversions, the *P* wave seismic velocity structure was assumed to be constant across this vertical plane. We chose our preferred seismic velocity model when the root-mean-square misfit was reduced to 135 ms, which corresponded to a scaled misfit χ^2 of 1.0. The discrepancies between picked and calculated traveltimes were quite evenly distributed between the earthquake and active-source data records (Appendix A).

5. Results

Our final compressional seismic velocity model (Figure 9) spans the plate boundary from the Taiwan Strait across central Taiwan into the Philippine Sea. Since we did not deploy OBSs in Taiwan Strait, we can only resolve the upper crustal structure here, but beneath the Coastal Plain, we image *P* wave seismic velocities of 7.0 km/s at 35 km depth. In the middle crust (25 km depth) of the Central Range the *P* wave seismic velocities are as low as 5.5 km/s, but they increase to 7.5 km/s at 55 km depth. This could be a good indication of Moho depth, but our only constraint here is the record of one earthquake at 65 km depth (Figure A3). The compressional seismic velocity structure of the Philippine Sea Plate is much different, resembling normal oceanic crust [e.g., *White et al*., 1992], with the exception of Gagua Ridge, where the crust appears thicker (Figure 9). A detailed interpretation of the tomographic image requires that we assess the resolution and compare our result with previous work on the crustal structure of central Taiwan.

Spatial variations in the fidelity of our seismic velocity model can be visualized using the resolution matrix [*Menke*, 1984], which we derive from the inverse matrix that produced our final result (Figure 9). In two resolution tests we calculate how much of an ellipse-shaped feature in the model can be recovered with the ray coverage provided by all the data of TAIGER transect T5 [*Van Avendonk et al*., 2004b]. We generally consider 0.5 to be adequately resolved. In our first test, we project an ellipse that is 16 km in width and 6 km in

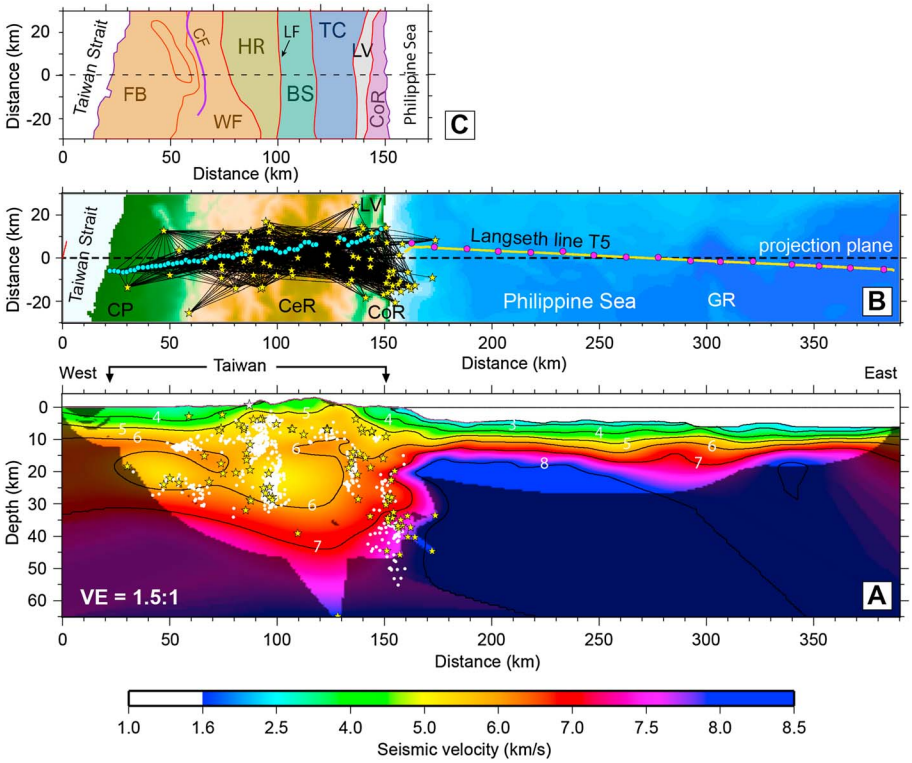

Figure 9. (a) Seismic velocity model produced by the 2-D tomographic inversion of active-source and earthquake traveltimes along transect T5. We do not have ray coverage from the TAIGER data in the shaded areas. Yellow stars mark the earthquakes used in this study, and white star indicates the location of the test shot. Seismicity between 2000 and 2009 within 15 km of the T5 profile is shown by white dots. (b) Projection of topography in the vicinity of T5. Raypaths between earthquakes and land seismometers are shown in black. CeR = Central Range; CoR = Coastal Range; CP = Coastal Plain; GR = Gagua Ridge; LV = Longitudinal Valley. (c) Map with geologic units of central Taiwan. BS = Backbone Slates; CF = Chelunpu Fault; FB = Foreland Basin; HR = Hsüehshan Range; LF = Lishan Fault; TC = Tananao Metamorphic Complex; WF = Western Foothills. VE = Vertical Exaggeration.

height on our model space. The resolution of such a small feature generally decreases with depth (Figure 10a), from 0.9 near the surface in the Western Foothills (at x = 90 km) to 0.3 at 25 km depth. We can therefore interpret such fine structure in the upper crust of most of Taiwan and the Philippine Sea Plate, but not in the Taiwan Strait. In a second test, we increase the size of the ellipse to 32 km by 12 km. The result (Figure 10b) shows that we can resolve such larger model features to a depth of at least 20 km in most of the model. Just offshore eastern Taiwan (at 160 km in our profile), we find a large lateral transition in crustal structure in the lower crust at 30–40 km depth (Figure 9). Unfortunately, the resolution here is less than 0.5 (Figure 10b). This area is sampled exclusively by rays between the deep earthquakes at the east coast and the TAIGER on-land stations. The one-sided illumination of the seismic velocity structure here requires that we must be careful interpreting this important detail of our model.

In our new analysis of transect T5, we incorporated previously unpublished OBS and onshore-offshore data, as well as earthquake traveltime data that were also used in the 3-D tomographic inversion of *Kuo-Chen et al.* [2012a]. It is therefore insightful to compare the two compressional seismic velocity models. Our new 2-D model (Figure 9) is overall less smooth than the 3-D model (Figure 11), which can be explained by the root-mean-square misfit between picked and calculated traveltimes, which was larger in the 3-D inversion (315 ms) [*Kuo-Chen et al.*, 2012a] than in the 2-D inversion (135 ms). The two models otherwise have similar structure in central Taiwan, but they differ significantly beneath eastern Taiwan and the Philippine Sea Plate. At 30 km depth beneath the Longitudinal Valley the *P* wave seismic velocity exceeds 7.5 km/s in *Kuo-Chen et al.* [2012a] 3-D model (Figure 11), while the seismic velocity in the 2-D model (Figure 9) is lower than 7.0 km/s here. This discrepancy is surprising, because both models are constrained by TAIGER earthquake data at these depths. We do not attribute the differences in seismic images in eastern Taiwan to the 2.5-D

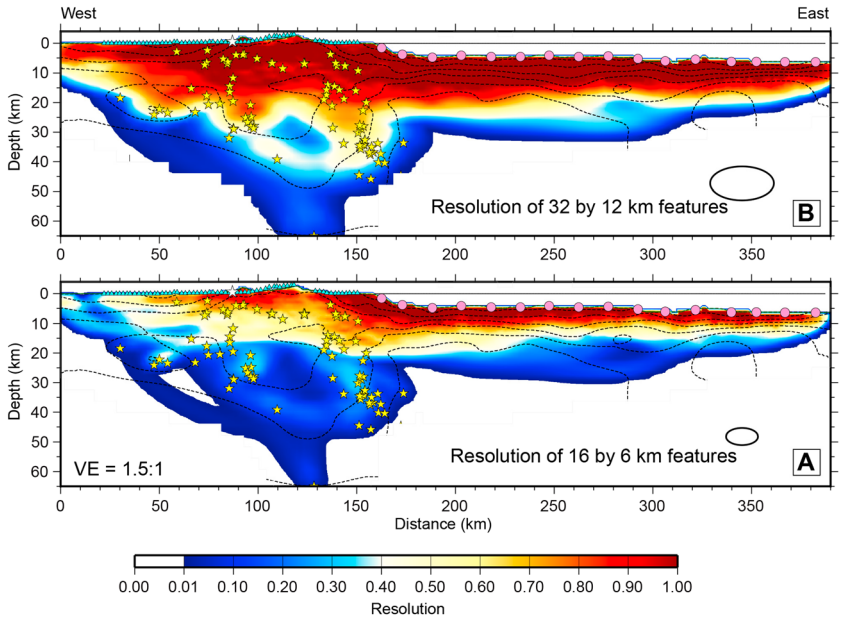

Figure 10. Resolution tests for two different length scales, calculated from the resolution matrix of the 2-D tomographic inversion. Dashed lines show the seismic velocity contours at 1.0 km/s intervals. Yellow stars mark the earthquakes used in the inversion. The white star shows the location of the test shot. Cyan triangles and pink circles show the land seismographs and OBSs, respectively. (a) Resolution of 16 km (horizontal) by 6 km (vertical) ellipse in the T5 profile. (b) Resolution of a 32 km (horizontal) by 12 km (vertical) ellipse.

inversion approach [*Van Avendonk et al.*, 2004a, 2004b]. We think that the variations in crustal structure along the strike of the plate boundary in central Taiwan are relatively small, such that we can invert for a 2-D seismic velocity model across Taiwan, as long as we use 3-D raypaths for the earthquake sources that lie up to 20 km north or south of the vertical plane through TAIGER line T5 (Figure 9b).

We consider the uneven and asymmetric raypath sampling of the seismic velocity deep crustal structure of eastern Taiwan a challenge in the interpretation of the resultant images. Our resolution tests (Figure 10) indicate that the deep crust beneath the east coast of Taiwan, at a distance of 151 km in our model, has good data coverage to a depth of 35 km. Nonetheless, this area lies outside the region where we have on-land TAIGER stations, which makes both the earthquake relocation and tomographic inversion less reliable. Interpretations of this important section of the model must therefore consider the possible trade-offs between seismic velocity structure and earthquake location. The deepest local earthquake in our new tomography study was 65 km (Figure A3). In contrast, the study by *Kuo-Chen et al.* [2012a] and several other authors [e.g., *Lallemand et al.*, 2013], used events to ~300 km depth, particularly along the east dipping plate boundary. The trade-off between seismic velocity structure and event location in the analyses of *Kuo-Chen et al.* [2012a] (Figure 11) and our study may therefore lead to different results, which may explain the difference in *P* wave seismic velocity structure at ~30 km depth beneath Longitudinal Valley (Figure 9).

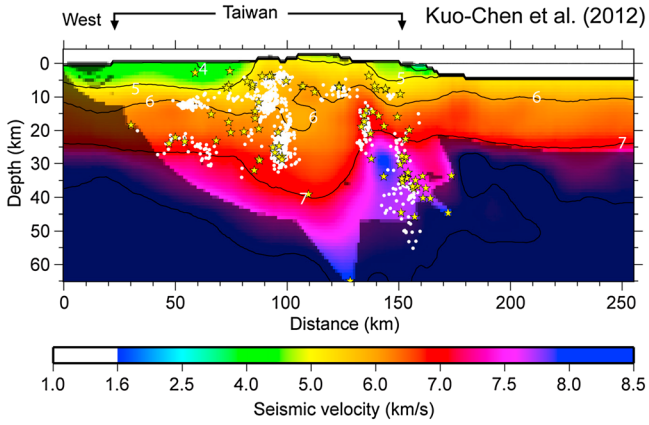

Figure 11. A vertical slice in the 3-D compressional seismic velocity model of *Kuo-Chen et al.* [2012a] along transect T5. Black contours at 1.0 km/s. The shading of the seismic velocity model is the same as in Figure 9. Yellow stars represent local earthquakes that were used in both tomographic studies. White dots mark seismicity between 2000 and 2009.

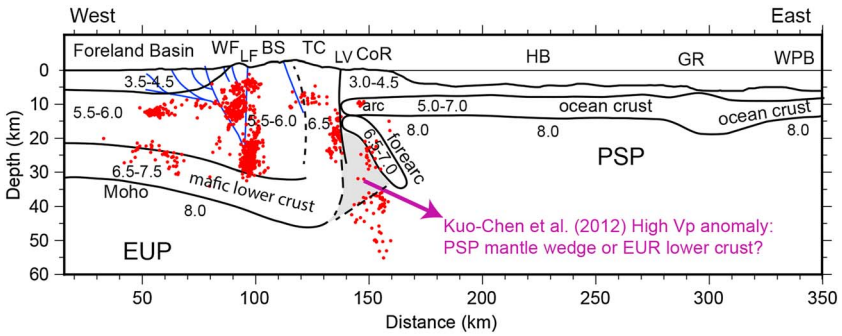

Figure 12. Interpretations of the 2-D seismic velocity structure along T5. Geographical abbreviations are explained in Figures 1 and 9. The 2-D seismic velocity model of Figure 9 and the 3-D seismic velocity model of *Kuo-Chen et al.* [2012a] (Figure 11) differ significantly between 135 km and 160 km. *Kuo-Chen et al.* [2012a] found seismic velocities exceeding 7.7 km/s (shaded area) at depths larger than 20 km, whereas our 2-D seismic velocity model (Figure 9) has velocities between 6.5 km/s and 7.5 km/s at this depth on the east coast of Taiwan. In either case this zone may represent a portion of the forearc mantle wedge of the Philippine Sea Plate. Lower seismic velocities would then suggest serpentinization due to infiltration of hydrous fluids from the South China Sea lithosphere that subducted here before the collision. Seismicity between 2000 and 2009 is shown in red. Interpretation of crustal faults in the vicinity of line T5 [*Brown et al.*, 2012] are shown in blue.

6. Discussion

A number of scientists have used either active-source or earthquake seismic data to produce *P* wave seismic velocity images of Taiwan and the surrounding oceans, since the deep structure of this region is of key importance for understanding arc-continent collision [*Roecker et al.*, 1987; *Hetland and Wu*, 1998; *Kim et al.*, 2005; *McIntosh et al.*, 2005; *Wu et al.*, 2007; *Kuo-Chen et al.*, 2012a; *Huang et al.*, 2014a, 2014b]. In controlled-source seismic experiments we can potentially obtain a dense traveltime data set across the plate boundary [*McIntosh et al.*, 2005], but it is difficult to interpret the nature of the lowermost crust in the resulting seismic velocity images if all sources and receivers are at the surface. Our new compressional seismic velocity model for TAIGER transect T5 (Figure 9), which we obtained from a 2-D inversion of both marine and land-based active-source and local earthquake seismic data, benefits from a high ray density at all crustal depths in Taiwan and on the Philippine Sea Plate.

6.1. Upper Crust and Sedimentary Basins

Along TAIGER transect T5, both the metamorphic grade [*Ho*, 1986; *Clark et al.*, 1993; *Beyssac et al.*, 2008] and the exhumation rates [*Liu et al.*, 2001; *Fuller et al.*, 2006] generally increase eastward from the Western Foothills to the continental basement of the eastern Central Range. Coincidentally, we see an increase in the compressional seismic velocity in the shallow subsurface along transect T5, from 4.0 km/s in the Western Foothills to 4.5 km/s in the Backbone Slate belt of the western Central Range, and to 5.0 km/s in the Tananao Complex of the eastern Central Range (Figure 9). Though some of the eastward increase in seismic velocity and metamorphic grade could be ascribed to deeper burial and exhumation during the Neogene arc-continent collision [*Simoes et al.*, 2007] (Figure 12), it is likely that the Tananao Complex reached peak metamorphism long before the arc-continent collision when these basement rocks were part of the stable continental crust of the Chinese margin [*Yamato et al.*, 2009]. The Tananao Complex also contains blocks of remnant South China Sea oceanic crust that were accreted to the wedge before the onset of collision [*Beyssac et al.*, 2008], which also contributes to the high *P* wave seismic velocity at the surface here on transect T5.

Much of the sediment that eroded from the Taiwan mountain belt was deposited along the west coast of Taiwan. In the western portion of our *P* wave seismic velocity model for transect T5 (Figure 9) the 5.0 km/s velocity contour may be a good local approximation of the depth to Miocene basement and a shallow east dipping detachment fault [*Brown et al.*, 2012; *Camanni et al.*, 2014] (Figure 12). This contour deepens eastward over a distance of 60 km from 5.0 km depth in the Taiwan Strait to 7.0 km depth beneath the Western Foothills, where it shallows over a distance of just 20 km to 2.0 km depth. The asymmetric shape of this basin north of Peikang Basement High (Figure 1) is typical for a foredeep, and it illustrates the interaction between flexure of the Eurasian Plate and accumulation of sediments that are shedding from the Taiwan orogen to the east [*Chou and Yu*, 2002; *Simoes and Avouac*, 2006; *Tensi et al.*, 2006].

The eastern end of transect T5 in the Philippine Sea lies just north of the trench axis on the toe of the sedimentary prism of the Ryukyu subduction system. Beneath the seafloor we imaged *P* wave seismic velocities lower than 3.0 km/s in sediments that must have been accreted to the overriding plate relatively recently. The deeper strata of the Philippine Sea Plate have higher seismic velocities, which is consistent with lower porosity due to increased compaction [*Erickson and Jarrard*, 1998]. The subduction of the high-standing Gagua Ridge has removed the front of the overriding prism at 300 km in our profile (Figure 2), such that some of these underlying sediments, with compressional velocities near 4.0 km/s are exposed at the seafloor (Figure 9). If the 5.0 km/s contour is a good approximation for the top of oceanic basement east of Taiwan, we estimate the combined thickness of the Huatung basin sediment cover and the toe of the overlying prism to vary between 5 km near the Luzon Arc and more than 8 km just west of Gagua Ridge. The sediment thickness is less than 5 km across the ridge, at the east end of transect T5.

6.2. Deformation of the Middle Crust

A fundamental problem in the interpretation of the style of crustal-scale deformation in Taiwan is the significance of the high level of seismicity between 8 km and 12 km depth across the mountain belt [*Carena et al*., 2002]. In principle, the zone of increased seismicity could represent a detachment surface [*Suppe*, 1981; *Yue et al*., 2005] that allows the middle and lower continental crust of the Eurasian Plate to underthrust the mountain belt at a shallow angle. Indeed, there is good evidence for such a shallow detachment zone in the Western Foothills [e.g., *Mouthereau et al*., 2002], but the shear zone may dip eastward to midcrustal depths beneath the Hsüehshan Range, if it even exists this far east [e.g., *Brown et al*., 2012]. In their study of the magnetotelluric data acquired during the TAIGER study, *Bertrand et al*. [2012] interpreted subvertical zones of high and low resistivity in the upper and middle crust to correlate with tectonic boundaries, such as the Lishan Fault. This interpretation is more consistent with uniform shortening of the crust beneath the Central Range (Figure 12) than with the thin-skinned tectonics of western Taiwan. In our new seismic velocity image of transect T5 (Figure 9), we find a compressional seismic wave speed of 5.5 km/s at 25 km depth beneath the Central Range. Together with the low V_P/V_S ratios imaged here by *Kuo-Chen et al*. [2012b], these low compressional seismic velocities suggest that quartz-rich upper crustal rocks and metasediments from the Eurasian Plate are buried in the orogen to depths greater than proposed by *Carena et al*. [2002]. Since the *P* wave seismic velocity is higher than 6.0 km/s at greater depth and farther east beneath the Tananao Complex (Figure 9), it appears that these silicic rocks are subsequently exhumed in the Hsüehshan Range and in the Backbone Slate belt before they enter the lower crust of the orogen. This interpretation is consistent with several kinematic models for the Taiwan orogen that are constrained by thermochronologic data and structural fabrics exposed across the mountain belt [*Willett et al*., 2003; *Fuller et al*., 2006; *Fisher et al*., 2007; *Simoes et al*., 2007].

If the Taiwan mountain belt is accommodating shortening by pure-shear contraction and thickening [*Yamato et al*., 2009] or by deep underplating of sedimentary and crystalline rocks [*Simoes et al*., 2007], dehydration of the incoming Eurasian strata may locally cause elevated fluid pressures that contribute to the low-velocity anomaly beneath the Central Range at a depth of 20–25 km (Figure 9). In addition, high erosion rates in the Central Range of Taiwan leads to upward advection of warm sedimentary rocks from these midcrustal depths, such that the temperature in the upper crust of the orogen is relatively high [*Lin*, 2000; *Rousset et al*., 2012]. Both the 5.5 km/s *P* wave velocities in this portion of our model, as well as the high seismic attenuation [*Lee et al*., 2010] support this interpretation (Figure 12). In the Southern Alps of New Zealand, a similar low-velocity zone in the middle crust has also been contributed to elevated temperatures and fluid pressure [*Stern et al*., 2001; *Van Avendonk et al*., 2004a]. As in the case of the Southern Alps, there is very little seismicity in the low seismic velocity anomaly east of the Hsüehshan Range and the Lishan Fault of Taiwan (Figure 9). However, at 7–12 km depth, where the seismic wave speed may be as high as 6.0 km/s, there is the band of higher seismicity that *Carena et al*. [2002] interpreted as a detachment fault. Alternatively, we suggest that the brittle-ductile transition lies near 10 km depth [*Kidder et al*., 2012] (Figure 12) and that the upper crust here is relatively strong due to surface cooling, such it can support larger earthquakes [*Sibson*, 1982]. At larger depth beneath the Central Range, seismicity is suppressed due to high temperatures and fluid pressures.

6.3. Lower Crust of Taiwan

The oblique angle of plate convergence in Taiwan implies that the arc-continent collision is more advanced in the north than in the south [*Suppe*, 1984; *Byrne et al*., 2011], which may explain large differences in the deep

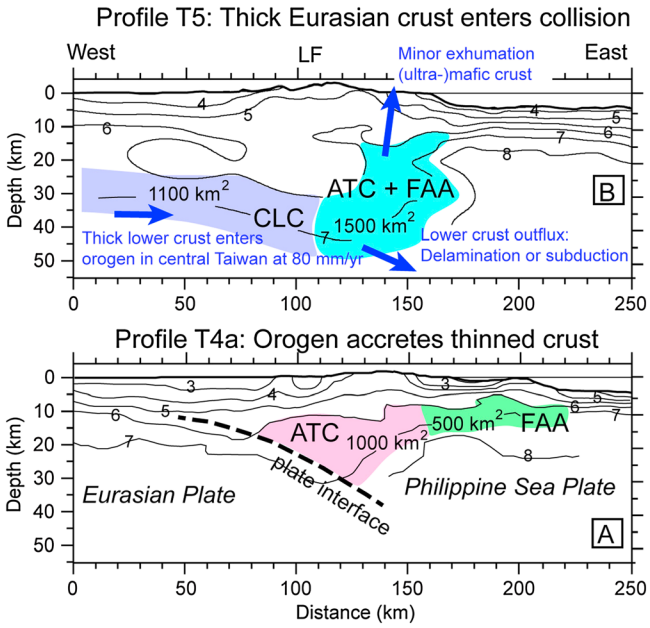

Figure 13. Comparison of two seismic velocity profiles from TAIGER transect T4a [*McIntosh et al.*, 2013] and transect T5 (this study). The location of these transects is shown in Figure 1. Four cross-sectional areas where the seismic velocity lies between 6.0 km/s and 7.5 km/s are highlighted in different colors. Thin black lines are seismic velocity contours spaced 1.0 km/s. (a) ATC = accreted transitional crust; FAA = forearc-arc block [*McIntosh et al.*, 2013]. (b) Seismic velocity structure of transect T5. Blue arrows indicate estimated flux of lower crustal rocks in and out of the orogen. CLC = continental lower crust; ATC + FAA = accreted transitional crust and forearc-arc block; LF = Lishan Fault.

crustal structure along the strike of the plate boundary. The Continental Margin Magnetic Anomaly (CMMA, outlined in pink in Figure 1) shows the seaward extend of thick Eurasian crust on the Chinese margin, projecting toward central Taiwan at the latitude of transect T5. Therefore, along TAIGER transect T4a only the thinned transitional crust of the rifted Chinese margin has entered the orogen [*McIntosh et al.*, 2013], but along T5 the accretion of the thinned crust was followed by a collision that involved the thick Eurasian crust of the Taiwan Strait. On transect T5, the orogen may have incorporated approximately 80 km more of the extended and intruded rifted margin crust than on transect T4a, where the CMMA still lies well west of the orogen. At a convergence rate of 80 mm/yr, this most landward section of the Eurasian rifted margin was consumed in roughly a million years. In Figure 13 we compare the compressional seismic velocity structure along transects T4a and T5 to examine how the structure of the lower crust has evolved during the arc-continent collision in southern Taiwan.

Along seismic refraction line T4a, the forearc was shortened in the incipient collision [*Lundberg et al.*, 1997], but the northern Luzon Arc platform still lies offshore, east of the Hengchun Peninsula (Figure 13a). In their seismic velocity image of this transect, *McIntosh et al.* [2013] used seismicity patterns to identify two distinct sections of crust with *P* wave seismic velocities between 6.0 km/s and 7.5 km/s: The material above the east dipping plate interface may be accreted blocks of extended crust from the rifted continental margin of the South China Sea. Along transect T4a, the forearc and arc block still appear to form a backstop to the growing prism to the west [*McIntosh et al.*, 2013]. Our tomographic image for T5 shows how ongoing contraction to the north in Taiwan has deformed both the Eurasian Plate and the Luzon Arc crust. At the east coast, the compressional seismic velocity is lower than 5.0 km/s in the upper 8 km of the Coastal Range (Figure 9), where fragments of the Luzon Volcanic Arc are interspersed with forearc and intraarc basin sediments [*Barrier and Angelier*, 1986; *Huang et al.*, 2001]. These *P* wave seismic velocities are much lower than what we expect for the crystalline basement of island arcs [*Calvert*, 2011]. It therefore appears that most of the Luzon Arc and Forearc crust resides at larger depth in the mountain belt, where the compressional seismic velocity is higher than 6.0 km/s. Compressional seismic velocities higher than 6.0 km/s or 6.5 km/s more likely represent mafic rocks, though large volumes of marble in the Tananao Complex of eastern Taiwan can also have such high seismic velocities [*Christensen and Mooney*, 1995]. Given that the *P* wave seismic velocity of both the arc crust and the accreted transitional crust of the Eurasian rifted margin [*McIntosh et al.*, 2013; *Lester et al.*, 2014] lies between 6.0 km/s and 7.5 km/s, we cannot distinguish these two units in our model for T5 (Figures 9 and 13).

In the arc-continent collision, thick crust of the Eurasian margin may have advanced as far as the Lishan Fault along transect T5 (Figure 13b). Therefore, a 10–15 km thick section of high-velocity lower crust has deformed into a broad crustal root between the Coastal Plain and the Lishan Fault of the Central Range of Taiwan (Figure 9). To the east, the accreted crust of the rifted margin still forms the eastern flank of the crustal root. The amount of high-velocity material, between 6.0 km/s and 7.5 km/s, in the crust of the mountain belt along T5 (Figure 13b) is approximately 1500 km^2, which is roughly the same as the combined size of the accreted

transitional crust and the arc and forearc block on transect T4a (Figure 13a). We therefore speculate that between transects T4a and T5, the influx of an 80 km wide stretch of rifted crust from the Eurasian Plate, mostly mafic material with a thickness of roughly 10 km [*Lester et al*., 2014], was balanced by a similar outflux due to delamination of the lower crust to the mantle at ~55 km depth [*Meissner and Mooney*, 1998]. Smaller amounts of mafic and ultramafic "transitional" crust from the Eurasian Plate are exhumed and eroded in the Tananao Complex of the eastern Central Range [*Beyssac et al*., 2008].

In central Taiwan, the orogen is evolving from a convergent margin that accretes Eurasian rifted margin crust that arrives from the west [*McIntosh et al*., 2013] to a larger mountain belt that also deforms the Philippine Sea Plate to the east. As the Luzon Arc underthrusts the mountain belt along the east coast in central Taiwan [*Barrier and Angelier*, 1986], it can no longer form a backstop to the growing wedge of accreted sediments and upper crustal rocks to the west. In our seismic velocity image for transect T5 (Figure 9) it appears that mafic rocks of the accreted, transitional crust form a new backstop in the eastern half of the orogen, which controls the exhumation of the less indurated rocks of the Hsüehshan Range and western Central Range (Backbone Range) to the west.

6.4. Fate of the Luzon Forearc Block

Possibly, the accretion of arc volcanic basement contributes to the continental crust of Taiwan as has been suggested [*Clift et al*., 2009], but at the latitude of transect T5 this process has started relatively recently. Approximately 50% of the 80 mm/yr oblique convergence between the Philippine Sea Plate and Eurasian Plate is accommodated near the suture at the Longitudinal Valley in central Taiwan [*Yu and Kuo*, 2001]. The active shear zone between the plates is highlighted by seismicity in eastern Taiwan at all crustal depths [e.g., *Wu et al*., 2004]. Here the Luzon Arc and Forearc crustal block may not yet be fully incorporated in the Eurasian crust, but our seismic velocity image (Figure 9) shows that most of the arc crust does not lie at shallow depth beneath the Costal Range along transect T5, so it must have been deformed and pushed downward in the collision.

Compression across the forearc basin appears to have stacked part of the accretionary wedge on forearc basement southeast of Taiwan [*Chi et al*., 2003]. Similarly, the southern portion of the Central Range may overthrust the forearc on the Hengchun Peninsula [*Shyu et al*., 2011]. The mode of deformation may be different farther north: Seismic velocity images and seismicity maps in southeastern Taiwan suggest that most of the convergence here is accommodated on east dipping thrust faults emerging just west of the Luzon Arc [*Lee et al*., 2001; *McIntosh et al*., 2005; *Huang et al*., 2014b]. It therefore seems that ongoing shortening in Taiwan caused the Philippine Sea Plate to fail along the island arc, where the lithosphere is thinner [*Chemenda et al*., 2001], and that the arc is now overriding the forearc block to the west. Along TAIGER transect T5 in central Taiwan, accreted arc volcanic rocks of the Coastal Range are facing the Asian basement rocks of the eastern Central Range across the Longitudinal Valley. Since we find *P* wave seismic velocities of ~7 km/s at 170 km in our model for transect T5, which is 20 km off the east coast, and at 30 km depth (Figure 9), it is possible that some of the thrusted forearc crust lies deep beneath the Philippine Sea Plate here (Figure 12). Unfortunately, the resolution is not good in this portion of the model for transect T5 (Figure 10), and the seismic image is locally very dependent on traveltimes from a few earthquakes offshore Taiwan whose location may not be uniquely determined (Figure 7).

If we compare our seismic velocity model with a few other recent tomography studies, we also find significant differences in the deep structure of eastern Taiwan. Our seismic velocity model (Figure 9), as well as previous work by *McIntosh et al*. [2005] and *Wu et al*. [2007] indicate that the crust beneath the Longitudinal Valley is approximately 40 km thick, but other seismic tomography studies [*Cheng et al*., 2002; *Kuo-Chen et al*., 2012a; *Lallemand et al*., 2013] found mantle *P* wave seismic velocities (>7.5 km/s) here at depths of 25 to 30 km (Figure 11). *Kuo-Chen et al*. [2012a] used a much larger number of earthquakes, and deeper events, recorded by the TAIGER array of land stations compared to our new study, which improved their ray coverage at large depth. On the other hand, *Kuo-Chen et al*. [2012a] did not include the OBS refraction data (Figure 4) and onshore-offshore active-source seismic data (Figure 5), which would be necessary to constrain the structure of the Philippine Sea Plate lithosphere. A potential problem in all these studies is that the origin time and location of earthquakes off the east coast of Taiwan are not well constrained by land-based seismometer arrays (Figure 7). The difference between our model (Figure 9) and that of *Kuo-Chen et al*. [2012a] (Figure 11) may therefore be explained in part by the possible trade-off between seismic velocity structure and earthquake relocation parameters.

The 7.5–8.0 km/s *P* wave seismic velocities beneath the Longitudinal Valley imaged by *Kuo-Chen et al*. [2012a] (Figure 11) could be interpreted as a piece of remnant forearc mantle, if the forearc block is indeed thrusted beneath the Luzon Arc in the collision with the Chinese margin (Figure 12). Since the tip of the forearc mantle wedge is hydrated and serpentinized in many subduction zones [*Hyndman and Peacock*, 2003], we think that this interpretation can also be applied to our new seismic velocity model (Figure 9). Some of the ~7.0 km/s *P* wave seismic velocities at ~30 km depth beneath the east coast of Taiwan (Figure 9) could represent a portion of the Luzon Forearc mantle that is ~30% serpentinized, which would have a density of 3100 kg/m^3 [*Christensen*, 2004]. A recent seismic tomography study of southern Taiwan shows *P* wave seismic velocities lower than 7.0 km/s beneath the Luzon Forearc crust here [*Cheng et al*., 2012], which makes it likely that the mantle wedge was hydrated farther north as well, and that serpentinites form a fraction of the crustal root of the Taiwan mountain belt beneath the suture of the Eurasian and Philippine Sea Plates.

7. Conclusions

We have carried out a joint inversion of earthquake and active-source seismic data to image the seismic velocity structure along TAIGER transect T5, across central Taiwan. Our analysis and interpretation of the new seismic velocity model for this transect leads us to the following conclusions:

1. For active-source seismic experiments in regions of high seismogenic activity, local earthquakes recorded into active-source recording arrays can significantly improve the data coverage in a tomographic analysis. In the case of a 2-D active-source seismic data set, such as transect T5 of the TAIGER project, local earthquakes can be included by 3-D ray tracing and 2-D inversions for seismic velocity structure. The contribution of the earthquakes can be significant, particularly if the number of active sources is limited due to budgetary, logistical, or regulatory factors. While their locations and origin times need to be determined as best as possible, these natural events can expand lateral and depth coverage and provide numerous crossing paths in orientations not provided by active sources on the Earth's surface.
2. The combined data set of TAIGER transect T5 documents the spatial variation in crustal structure across the Taiwan mountain belt. We find that the Moho depth increases from ~30 km beneath the western coastal plain to approximately 55 km beneath the Central Range of Taiwan, which requires significant thickening of the incoming continental crust. The *P* wave seismic velocities in the middle crust are as low as 5.5 km/s at ~25 km depth, which suggests that upper crustal rocks and sediments from the Eurasian Plate are underthrusting the Central Range to these depths. As a result, it is unlikely that a shallow, east dipping detachment extends across the island. Instead, much of the contraction of the crust across the plate boundary appears to be taken up by uniform shortening and thickening of the entire crust.
3. Along the east coast of central Taiwan, the Luzon Arc and Forearc crust are strongly deformed and likely detached from the Philippine Sea Plate. The *P* wave seismic velocities in the Coastal Range in eastern Taiwan are lower than 4.0 km/s in the upper 5 km beneath the surface, but increase to more than 6.0 km/s at 20 km depth. Though arc volcanic rocks are outcropping in the Coastal Range, it is likely that most of the arc basement resides in the middle crust in eastern Taiwan.
4. In central and eastern Taiwan we find a crustal root with *P* wave seismic velocities between 6.0 and 7.5 km/s, which is consistent with a mafic average composition. In southern Taiwan, *McIntosh et al*. [2013] interpreted a high-velocity anomaly in the incipient collision zone, which they attributed to the accretion of rifted margin crust. Since the volume of high-velocity lower crust does not appear to grow with ongoing convergence between the Eurasian and Philippine Sea Plates in central Taiwan, we speculate that some of the mafic lower crust of the orogen is lost by delamination or subduction into the deeper mantle.

Appendix A: Ray Diagrams

In the tomography analysis we iterated steps of ray tracing and linearized inversion [*Van Avendonk et al*., 2004b]. After we found a seismic velocity model that fits the traveltime constraints, we traced rays in the final model to show the model coverage and data fits for a select number of instruments. In Figure A1 the ray diagram for several OBSs shows that the seismic refractions provided even coverage to a depth of approximately 15 km beneath sea level. The number of traveltime picks that we were able to fit along the OBS

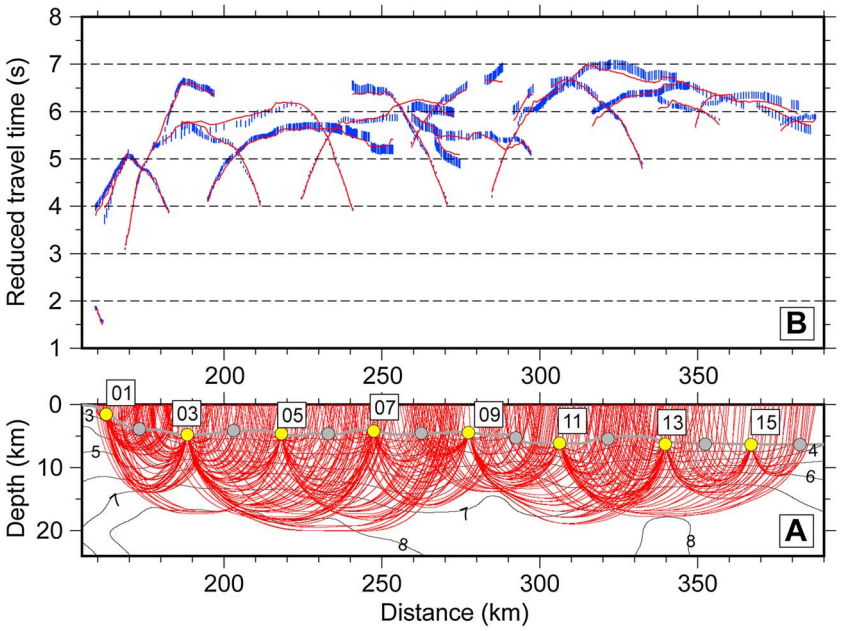

Figure A1. (a) Raypaths (red) between air gun shots and a select number of OBSs (yellow circles) on transect T5 off eastern Taiwan. Other OBSs shown in gray. Contours represent the seismic velocities determined by the tomographic inversion. (b) Traveltime picks for selected OBSs (blue, with error bars) and traveltimes calculated (red) in our final seismic velocity model. Traveltime axis is reduced by 7 km/s.

shot line was very consistent. The data fit for the onshore-offshore stations was also good (Figure A2), but the ray coverage that these data provide is not reversed beneath central Taiwan. At the east coast of Taiwan, the crossing raypaths between source-receiver pairs sample the seismic velocity structure to a depth of approximately 18 km (Figure A2). The source-receiver geometry for the earthquake traveltimes complements the constraints from the active-source seismic data set very well, and the data fit of these local earthquakes is generally good (Figure A3).

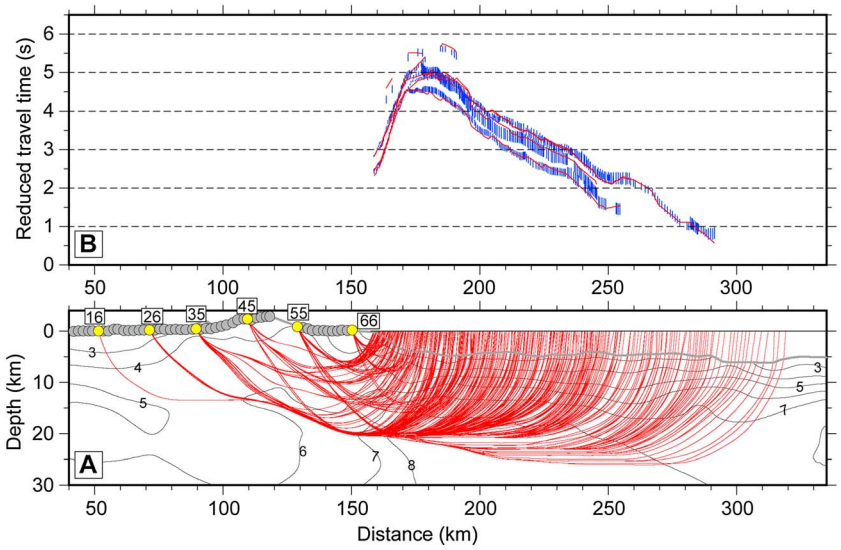

Figure A2. (a) Raypaths (red) between air gun shots off eastern Taiwan and a select number of onshore seismographs (yellow circles) on transect T5. Other stations are shown in gray. Contours represent the seismic velocities determined by the tomographic inversion. (b) Traveltime picks for selected stations (blue, with error bars) and traveltimes calculated (red) in our final seismic velocity model. Traveltime axis is reduced by 7 km/s.

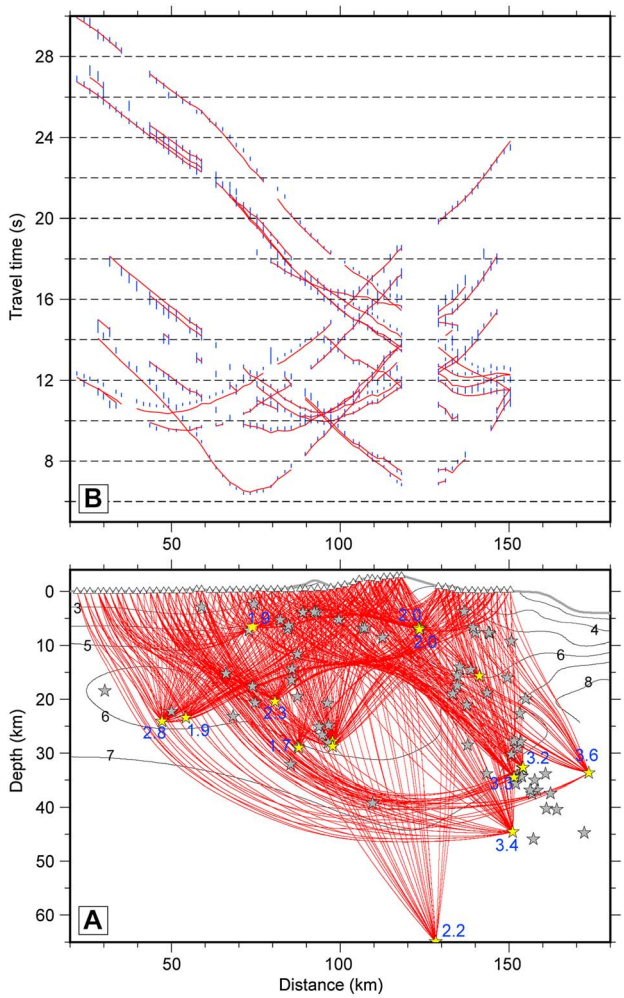

Figure A3. (a) Raypaths (red) between land stations (triangles) and a select number of earthquakes (yellow stars, their magnitude in blue label) projected on transect T5. Other earthquakes used in this study are shown in gray. Contours represent the seismic velocities determined by the tomographic inversion. (b) Traveltime picks for selected earthquakes (blue, with error bars) and traveltimes calculated (red) in our final seismic velocity model.

Acknowledgments

We thank the officers and crew of the science vessels that were used during TAIGER and the many scientists and students that participated in the fieldwork on land and at sea. The U.S. Ocean-Bottom Seismograph Instrument Pool (www.obsip.org), which is funded by the National Science Foundation, and the National Taiwan Ocean University OBS Group each provided eight instruments to record marine seismic refraction data on TAIGER transect T5. OBSIP data are archived at the IRIS Data Management Center (www.iris.edu). Land seismic instruments and field assistance were provided by IRIS/PASSCAL. We acknowledge the help of W.T. Liang and M.H. Shih of Academia Sinica with the extraction of some of the onshore-offshore seismic data. The TAIGER project was supported by the U.S. National Science Foundation Continental Dynamics Program (grant EAR-0408609) and by funding from the National Science Council and Ministry of the Interior in Taiwan. We thank the Associate Editor, T. Byrne, and an anonymous reviewer for comments and suggestions that led to improvements in the manuscript. This is UTIG contribution 2737.

References

Barrier, E., and J. Angelier (1986), Active collision in eastern Taiwan: The Coastal Range, *Tectonophysics*, *125*, 39–72, doi:10.1016/0040-1951(86)90006-5.

Bertrand, E. A., M. J. Unsworth, C. W. Chiang, C. S. Chen, C. C. Chen, F. T. Wu, E. Turkoglu, H. L. Hsu, and G. J. Hill (2012), Magnetotelluric imaging beneath the Taiwan orogen: An arc-continent collision, *J. Geophys. Res.*, *117*, B01402, doi:10.1029/2011JB008688.

Beyssac, O., M. Simoes, J. P. Avouac, K. A. Farley, Y. G. Chen, Y. C. Chan, and B. Goffé (2007), Late Cenozoic metamorphic evolution and exhumation of Taiwan, *Tectonics*, *26*, TC6001, doi:10.1029/2006TC002064.

Beyssac, O., F. Negro, M. Simoes, Y. C. Chan, and Y. G. Chen (2008), High-pressure metamorphism in Taiwan: From oceanic subduction to arc-continent collision?, *Terra Nova*, *20*, 118–125, doi:10.1111/j.1365-3121.2008.00796.x.

Brown, D., J. Alvarez-Marron, M. Schimmel, Y.-M. Wu, and G. Camanni (2012), The structure and kinematics of the central Taiwan mountain belt derived from geological and seismicity data, *Tectonics*, *31*, TC5013, doi:10.1029/2012TC003156.

Byrne, T., Y.-C. Chan, R.-J. Rau, C. Y. Lu, Y. H. Lee, and Y. J. Wang (2011), The arc-continent collision in Taiwan, in *Arc-Continent-Collision, Frontiers in Earth Sciences*, edited by D. Brown and P. D. Ryan, pp. 213–245, Springer, Berlin.

Calvert, A. J. (2011), The seismic structure of island arc crust, in *Arc-Continent Collision, Frontiers in Earth Sciences*, edited by D. Brown and P. D. Ryan, pp. 87–119, Springer, Heidelberg.

Camanni, G., C.-H. Chen, D. Brown, J. Alvarez-Marron, Y.-M. Wu, H.-A. Chen, H.-H. Huang, H.-T. Chu, M.-M. Chen, and C.-H. Chang (2014), Basin inversion in central Taiwan and its importance for seismic hazard, *Geology*, *42*, 147–150, doi:10.1130/G35102.1.

Carena, S., J. Suppe, and H. Kao (2002), Active detachment of Taiwan illuminated by small earthquakes and its control of first-order topography, *Geology*, *30*, 935–938.

Chang, C. P., T. Y. Chang, J. Angelier, H. Kao, J. C. Lee, and S. B. Yu (2003), Strain and stress field in Taiwan oblique convergent system: Constraints from GPS observation and tectonic data, *Earth Planet. Sci. Lett.*, *214*, 115–127, doi:10.1016/S0012-821X(03)00360-1.

Chemenda, A. I., R.-K. Yang, J.-F. Stephan, E. A. Konstantinovskaya, and G. M. Ivanov (2001), New results from physical modelling of arc-continent collision in Taiwan: Evolutionary model, *Tectonophysics*, *333*, 159–178, doi:10.1016/S0040-1951(00)00273-0.

Cheng, W.-B., C. Wang, C.-T. Shyu, and T.-C. Shin (2002), Crustal structure of the convergent plate-boundary zone, eastern Taiwan, assessed by seismic tomography, in *Geology and Geophysics of an Arc-Continent Collision, Taiwan*, edited by T. B. Byrne and C.-S. Liu, pp. 161–175, *Geol. Soc. Am. Spec. Pap.*, *358*, Boulder, Colo.

Cheng, W. B. (2004), Crustal structure of the high magnetic anomaly belt, Western Taiwan, and its implications for continental margin deformation, *Mar. Geophys. Res.*, *25*(1–2), 79–93, doi:10.1007/s11001-005-0735-3.

Cheng, W. B., S. K. Hsu, and C. H. Chang (2012), Tomography of the southern Taiwan subduction zone and possible emplacement of crustal rocks into the forearc mantle, *Global Planet. Change*, *90-91*, 20–28, doi:10.1016/j.gloplacha.2012.01.003.

Chi, W.-C., D. L. Reed, G. Moore, T. Nguyen, C.-S. Liu, and N. Lundberg (2003), Tectonic wedging along the rear of the offshore Taiwan accretionary prism, *Tectonophysics*, *374*, 199–217, doi:10.1016/j.tecto.2003.08.004.

Ching, K.-E., K. M. Johnson, R.-J. Rau, R. Y. Chuang, L.-C. Kuo, and P.-L. Leu (2011), Inferred fault geometry and slip distribution of the 2010 Jiashian, Taiwan, earthquake is consistent with a thick-skinned deformation model, *Earth Planet. Sci. Lett.*, *301*, 78–86, doi:10.1016/j.epsl.2010.10.021.

Chou, Y.-W., and H.-S. Yu (2002), Structural expressions of flexural extension in the arc-continent collisional foredeep of western Taiwan, in *Geology and Geophysics of an Arc-Continent Collision, Taiwan*, edited by T. B. Byrne and C.-S. Liu, *Geol. Soc. Am. Spec. Pap.*, *358*, 1–12, Boulder, Colo.

Christensen, N. I. (2004), Serpentinites, peridotites, and seismology, *Int. Geol. Rev.*, *46*, 795–816, doi:10.2747/0020-6814.46.9.795.

Christensen, N. I., and W. D. Mooney (1995), Seismic velocity structure and composition of the continental crust: A global view, *J. Geophys. Res.*, *100*, 9761–9788, doi:10.1029/95JB00259.

Chuang, R. Y., K. M. Johnson, Y.-M. Wu, K.-E. Ching, and L.-C. Kuo (2013), A midcrustal ramp-fault structure beneath the Taiwan tectonic wedge illuminated by the 2013 Nantou earthquake series, *Geophys. Res. Lett.*, *40*, 5080–5084, doi:10.1002/grl.51005.

Clark, M. B., D. M. Fisher, C. Y. Lu, and C. H. Chen (1993), Kinematic analyses of the Hsüehshan Range, Taiwan: A large-scale pop-up structure, *Tectonics*, *12*, 205–217, doi:10.1029/92TC01711.

Clift, P. D., A. T. S. Lin, F. Wu, A. E. Draut, T.-H. Lai, L.-Y. Fei, H. Schouten, and L. Teng (2008), Post-collisional collapse in the wake of migrating arc-continent collision in the Ilan Basin, Taiwan, in *Formation and Applications of the Sedimentary Record in Arc Collision Zones*, edited by A. E. Draut, P. D. Clift, and D. W. Scholl, *Geol. Soc. Am. Spec. Pap.*, *436*, 257–278, Boulder, Colo.

Clift, P. D., H. Schouten, and P. Vannucchi (2009), Arc-continent collisions, sediment recycling and the maintenance of the continental crust, in *Earth Accretionary Systems in Space and Time*, edited by P. A. Cawood and A. Kröner, *Geol. Soc. Spec. Publ.*, *318*, 75–103, London.

DeBari, S. M., and A. R. Greene (2011), Vertical stratification of composition, density, and inferred magmatic processes in exposed arc crustal sections, in *Arc-Continent Collision, Frontiers in Earth Sciences*, edited by D. Brown and P. D. Ryan, pp. 121–144, Springer, Berlin.

Deffontaines, B., O. Lacombe, J. Angelier, H. T. Chu, F. Mouthereau, C. T. Lee, J. Deramond, J. F. Lee, M. S. Yu, and P. M. Liew (1997), Quaternary transfer faulting in the Taiwan Foothills: Evidence from a multisource approach, *Tectonophysics*, *274*(1–3), 61–82, doi:10.1016/s0040-1951(96)00298-3.

Draut, A. E., and P. D. Clift (2013), Differential preservation in the geologic record of intraoceanic arc sedimentary and tectonic processes, *Earth Sci. Rev.*, *116*, 57–84, doi:10.1016/j.earscirev.2012.11.003.

Eakin, D. H., K. D. McIntosh, H. J. A. Van Avendonk, L. Lavier, R. Lester, C.-S. Liu, and C.-S. Lee (2014), Crustal-scale seismic profiles across the Manila subduction zone: The transition from intraoceanic subduction to incipient collision, *J. Geophys. Res. Solid Earth*, *119*, 1–17, doi:10.1002/2013JB010395.

Erickson, S. N., and R. D. Jarrard (1998), Velocity-porosity relationships for water-saturated siliciclastic sediments, *J. Geophys. Res.*, *103*, 30,385–30,406, doi:10.1029/98JB02128.

Ernst, W. G. (1981), Petrotectonic settings of glaucophane schist belts and some implications for Taiwan, *Geol. Soc. China Mem.*, *4*, 229–267.

Fisher, D. M., S. Willett, Y. En-Chao, and M. B. Clark (2007), Cleavage fronts and fans as reflections of orogen stress and kinematics in Taiwan, *Geology*, *35*, 65–68, doi:10.1130/g22850a.1.

Fuller, C. W., S. D. Willett, D. Fisher, and C. Y. Lu (2006), A thermomechanical wedge model of Taiwan constrained by fission-track thermochronometry, *Tectonophysics*, *425*, 1–24.

Hall, R. (2009), The Eurasian SE Asian margin as a modern example of an accretionary orogen, in *Earth Accretionary Systems in Space and Time*, edited by P. A. Cawood and A. Kröner, *Geol. Soc. Spec. Publ.*, *318*, 351–372, London.

Hetland, E. A., and F. T. Wu (1998), Deformation of the Philippine Sea Plate under the Coastal Range, Taiwan: Results from an offshore-onshore seismic experiment, *Terr. Atmos. Oceanic Sci.*, *9*, 363–378.

Ho, C. S. (1986), A synthesis of the geologic evolution of Taiwan, *Tectonophysics*, *125*(1–3), 1–16, doi:10.1016/0040-1951(86)90004-1.

Holbrook, W. S., D. Lizarralde, S. McGeary, N. Bangs, and J. Diebold (1999), Structure and composition of the Aleutian island arc and implications for continental crustal growth, *Geology*, *27*, 31–34.

Huang, C. Y., K. Y. Xia, P. B. Yuan, and P. G. Chen (2001), Structural evolution from Paleogene extension to Latest Miocene-Recent arc-continent collision offshore Taiwan: Comparison with on land geology, *J. Asian Earth Sci.*, *19*, 619–639, doi:10.1016/S1367-9120(00)00065-1.

Huang, C.-Y., W.-Y. Wua, C.-P. Chang, S. Tsao, P. B. Yuan, C.-W. Lin, and K.-Y. Xia (1997), Tectonic evolution of accretionary prism in the arc-continent collision terrane of Taiwan, *Tectonophysics*, *281*, 31–51, doi:10.1016/S0040-1951(97)00157-1.

Huang, H.-H., Y.-M. Wu, X. Song, C.-H. Chang, H. Kuo-Chen, and S.-J. Lee (2014a), Investigating the lithospheric velocity structures beneath the Taiwan region by nonlinear joint inversion of local and teleseismic P wave data: Slab continuity and deflection, *Geophys. Res. Lett.*, *41*, 6350–6357, doi:10.1002/2014GL061115.

Huang, H.-H., Y.-M. Wu, X. Song, C.-H. Chang, S.-J. Lee, T.-M. Chang, and H.-H. Hsieh (2014b), Joint Vp and Vs tomography of Taiwan: Implications for subduction-collision orogeny, *Earth Planet. Sci. Lett.*, *392*, 177–191, doi:10.1016/j.epsl.2014.02.026.

Hyndman, R. D., and S. M. Peacock (2003), Serpentinization of the forearc mantle, *Earth Planet. Sci. Lett.*, *212*, 417–432, doi:10.1016/S0012-821X(03)00263-2.

Jagoutz, O., and M. D. Behn (2013), Foundering of lower island-arc crust as an explanation for the origin of the continental Moho, *Nature*, *504*, 131–134, doi:10.1038/nature12758.

Jull, M., and P. B. Kelemen (2001), On the conditions for lower crustal convective instability, *J. Geophys. Res.*, *106*, 6423–6446, doi:10.1029/2000JB900357.

Kidder, S., J.-P. Avouac, and Y.-C. Chan (2012), Constraints from rocks in the Taiwan orogen on crustal stress levels and rheology, *J. Geophys. Res.*, *117*, B09408, doi:10.1029/2012JB009303.

Kim, K.-H., J.-M. Chiu, J. Pujol, K.-C. Chen, B.-S. Huang, Y.-H. Yeh, and P. Shen (2005), Three-dimensional Vp and Vs structural models associated with the active subduction and collision tectonics in the Taiwan region, *Geophys. J. Int.*, *162*, 204–220.

Kuo-Chen, H., F. T. Wu, and S. W. Roecker (2012a), Three-dimensional P velocity structures of the lithosphere beneath Taiwan from the analysis of TAIGER and related seismic data sets, *J. Geophys. Res.*, *117*, B06306, doi:10.1029/2011JB009108.

Kuo-Chen, H., F. T. Wu, D. M. Jenkins, J. Mechie, S. W. Roecker, C.-Y. Wang, and B.-S. Huang (2012b), Seismic evidence for the α-β quartz transition beneath Taiwan from Vp/Vs tomography, *Geophys. Res. Lett.*, *39*, L22302, doi:10.1029/2012GL053649.

Lallemand, S., Y. Font, H. Bijwaard, and H. Kao (2001), New insights on 3-D plates interaction from tomography and tectonic implications, *Tectonophysics*, *335*, 229–253.

Lallemand, S., T. Theunissen, P. Schnürle, C.-S. Lee, C.-S. Liu, and Y. Font (2013), Indentation of the Philippine Sea Plate by the Eurasia Plate in Taiwan: Details from recent marine seismological experiments, *Tectonophysics*, *594*, 60–79, doi:10.1016/j.tecto.2013.03.020.

Lan, C.-Y., C.-S. Lee, T.-F. Yui, H.-T. Chu, and B.-M. Jahn (2008), The tectono-thermal events of Taiwan and their relationship with SE China, *Terr. Atmos. Oceanic Sci.*, *19*, 257–278, doi:10.3319/TAO.2008.19.3.257(TT).

Lee, C.-P., N. Hirata, B.-S. Huang, W.-G. Huang, and Y.-B. Tsai (2010), Evidence of a highly attenuative aseismic zone in the active collision orogen of Taiwan, *Tectonophysics*, *489*, 128–138, doi:10.1016/j.tecto.2010.04.009.

Lee, J. C., J. Angelier, H. T. Chu, J. C. Hu, and F. S. Jeng (2001), Continuous monitoring of an active fault in a plate suture zone: A creepmeter study of the Chihshang active fault, eastern Taiwan, *Tectonophysics*, *333*, 219–240, doi:10.1016/S0040-1951(00)00276-6.

Lee, T. Y., and L. A. Lawver (1995), Cenozoic plate reconstruction of Southeast Asia, *Tectonophysics*, *251*, 85–138, doi:10.1016/0040-1951(95)00023-2.

Lester, R., and K. McIntosh (2012), Multiple attenuation in crustal-scale imaging: Examples from the TAIGER marine reflection data set, *Mar. Geophys. Res.*, *33*, 289–305.

Lester, R., L. L. Lavier, K. McIntosh, H. J. A. Van Avendonk, and F. Wu (2012), Active extension in Taiwan's pre-collision zone: A new model of plate-bending in continental crust, *Geology*, *40*, 831–834, doi:10.1130/G33142.1.

Lester, R., K. McIntosh, H. J. A. Van Avendonk, L. Lavier, C.-S. Liu, and T. K. Wang (2013), Crustal accretion in the Manila trench accretionary wedge at the transition from subduction to mountain-building in Taiwan, *Earth Planet. Sci. Lett.*, *375*, 430–440, doi:10.1016/j.epsl.2013.06.007.

Lester, R., H. J. A. Van Avendonk, K. McIntosh, L. Lavier, C.-S. Liu, T. K. Wang, and F. Wu (2014), Rifting and magmatism in the northeastern South China Sea from wide-angle tomography and seismic reflection imaging, *J. Geophys. Res. Solid Earth*, *119*, 2305–2323, doi:10.1002/2013JB010639.

Lin, A. T., and A. B. Watts (2002), Origin of the West Taiwan basin by orogenic loading and flexure of a rifted continental margin, *J. Geophys. Res.*, *107*(B9), 2185, doi:10.1029/2001JB000669.

Lin, A. T., A. B. Watts, and S. Hesselbo (2003), Cenozoic stratigraphy and subsidence history of the South China Sea margin in the Taiwan region, *Basin Res.*, *15*, 453–478.

Lin, C. H. (2002), Active continental subduction and crustal exhumation: The Taiwan orogeny, *Terra Nova*, *14*, 281–287, doi:10.1046/j.1365-3121.2002.00421.x.

Lin, C.-H. (2000), Thermal modeling of continental subduction and exhumation constrained by heat flow and seismicity in Taiwan, *Tectonophysics*, *324*, 189–201, doi:10.1016/S0040-1951(00)00117-7.

Liu, T. K., S. Hsieh, Y. G. Chen, and W. S. Chen (2001), Thermo-kinematic evolution of the Taiwan oblique-collision mountain belt as revealed by zircon fission track dating, *Earth Planet. Sci. Lett.*, *186*(1), 45–56, doi:10.1016/s0012-821x(01)00232-1.

Lundberg, N., D. L. Reed, C.-S. Liu, and J. Lieske (1997), Forearc-basin closure and arc accretion in the submarine suture zone south of Taiwan, *Tectonophysics*, *274*, 5–23, doi:10.1016/S0040-1951(96)00295-8.

Malavieille, J., S. Lallemand, S. Dominguez, A. Deschamps, C.-Y. Lu, C.-S. Liu, and P. Schnürle (2002), Arc-continent collision in Taiwan: New marine observations and tectonic evolution, in *Geology and Geophysics of an Arc-Continent Collision, Taiwan*, edited by T. B. Byrne and C.-S. Liu, *Geol. Soc. Am. Spec. Pap.*, *358*, 187–211, Boulder, Colo.

McIntosh, K., Y. Nakamura, T.-K. Wang, R.-C. Shih, A. Chen, and C.-S. Liu (2005), Crustal-scale seismic profiles across Taiwan and the western Philippine Sea, *Tectonophysics*, *401*, 23–54, doi:10.1016/j.tecto.2005.02.015.

McIntosh, K., H. van Avendonk, L. Lavier, W. R. Lester, D. Eakin, F. Wu, C.-S. Liu, and C.-S. Lee (2013), Inversion of a hyper-extended rifted margin in the southern Central Range of Taiwan, *Geology*, *41*, 871–874, doi:10.1130/G34402.1.

McLennan, S. M., and S. R. Taylor (1982), Geochemical constraints on the growth of the continental crust, *J. Geol.*, *90*, 347–361.

Meissner, R., and W. Mooney (1998), Weakness of the lower continental crust: A condition for delamination, uplift, and escape, *Tectonophysics*, *296*(1–2), 47–60, doi:10.1016/s0040-1951(98)00136-x.

Menke, W. (1984), *Geophysical Data Analysis: Discrete Inverse Theory*, 289 pp., Academic Press, San Diego, Calif.

Moser, T. J. (1991), Shortest path calculation of seismic rays, *Geophysics*, *56*, 59–67, doi:10.1190/1.1442958.

Moser, T. J., G. Nolet, and R. K. Snieder (1992), Ray bending revisited, *Bull. Seismol. Soc. Am.*, *82*, 259–288.

Mouthereau, F., and C. Petit (2003), Rheology and strength of the Eurasian continental lithosphere in the foreland of the Taiwan collision belt: Constraints from seismicity, flexure, and structural styles, *J. Geophys. Res.*, *108*(B11), 2512, doi:10.1029/2002JB002098.

Mouthereau, F., and O. Lacombe (2006), Inversion of the Paleogene Chinese continental margin and thick-skinned deformation in the Western Foreland of Taiwan, *J. Struct. Geol.*, *28*, 1977–1993, doi:10.1016/j.jsg.2006.08.007.

Mouthereau, F., B. Deffontaines, O. Lacombe, and J. Angelier (2002), Variations along the strike of the Taiwan thrust belt: Basement control on structural style, wedge geometry, and kinematics, in *Geology and Geophysics of an Arc-Continent Collision, Taiwan*, edited by T. B. Byrne and C.-S. Liu, *Geol. Soc. Am. Spec. Pap.*, *358*, 31–54, Boulder, Colo.

Mouthereau, F., A. B. Watts, and E. Burov (2013), Structure of orogenic belts controlled by lithosphere age, *Nat. Geosci.*, *6*, 785–789, doi:10.1038/ngeo1902.

Roecker, S. W., Y. H. Yeh, and Y. B. Tsai (1987), Three-dimensional P and S wave velocity structures beneath Taiwan—Deep structure beneath an arc-continent collision, *J. Geophys. Res.*, *92*, 10,547–10,570, doi:10.1029/JB092iB10p10547.

Rousset, B., S. Barbot, J.-P. Avouac, and Y.-J. Hsu (2012), Postseismic deformation following the 1999 Chi-Chi earthquake, Taiwan: Implication for lower-crust rheology, *J. Geophys. Res.*, *117*, B12405, doi:10.1029/2012JB009571.

Sengör, A. M. C., B. A. Natal'in, and V. S. Burtman (1993), Evolution of the Altaid tectonic collage and Palaeozoic crustal growth in Eurasia, *Nature*, *364*, 299–307, doi:10.1038/364299a0.

Shillington, D. J., H. J. A. Van Avendonk, W. S. Holbrook, P. B. Kelemen, and M. J. Hornbach (2004), Composition and structure of the central Aleutian island arc from arc-parallel wide-angle seismic data, *Geochem. Geophys. Geosyst.*, *5*, Q10006, doi:10.1029/2004GC000715.

Shyu, J. B. H., Y. M. Wu, C. H. Chang, and H. H. Huang (2011), Tectonic erosion and the removal of forearc lithosphere during arc-continent collision: Evidence from recent earthquake sequences and tomography results in eastern Taiwan, *J. Asian Earth Sci.*, *42*, 415–422, doi:10.1016/j.jseaes.2011.05.015.

Sibson, R. H. (1982), Fault zone models, heat flow, and the depth distribution of earthquakes in the continental crust of the United States, *Bull. Seismol. Soc. Am.*, *72*, 151–163.

Simoes, M., and J. P. Avouac (2006), Investigating the kinematics of mountain building in Taiwan from the spatiotemporal evolution of the foreland basin and western foothills, *J. Geophys. Res.*, *111*, B10401, doi:10.1029/2005JB004209.

Simoes, M., J. P. Avouac, O. Beyssac, B. Goffe, K. A. Farley, and Y. G. Chen (2007), Mountain building in Taiwan: A thermokinematic model, *J. Geophys. Res.*, *112*, B11405, doi:10.1029/2006JB004824.

Stern, T., S. Kleffmann, D. Okaya, M. Scherwath, and S. Bannister (2001), Low seismic-wave speeds and enhanced fluid pressure beneath the Southern Alps of New Zealand, *Geology*, *29*, 679–682.

Stolar, D. B., S. D. Willett, and D. R. Montgomery (2007), Characterization of topographic steady state in Taiwan, *Earth Planet. Sci. Lett.*, *261*, 421–431, doi:10.1016/j.epsl.2007.07.045.

Suppe, J. (1981), Mechanics of mountain building and metamorphism in Taiwan, *Mem. Geol. Soc. China*, *4*, 67–89.

Suppe, J. (1984), Kinematics of arc-continent collision, flipping of subduction, and backarc spreading near Taiwan, *Mem. Geol. Soc. China*, *6*, 21–33.

Tatsumi, Y., H. Shukuno, K. Tani, N. Takahashi, S. Kodaira, and T. Kogiso (2008), Structure and growth of the Izu-Bonin-Mariana Arc crust: 2. Role of crust-mantle transformation and the transparent Moho in arc crust evolution, *J. Geophys. Res.*, *113*, B02203, doi:10.1029/2007JB005121.

Teng, L. S. (1990), Geotectonic evolution of late Cenozoic arc–continent collision in Taiwan, *Tectonophysics*, *183*, 57–76, doi:10.1016/0040-1951(90)90188-E.

Teng, L. S. (1996), Extensional collapse of the northern Taiwan mountain belt, *Geology*, *24*, 949–952.

Tensi, J., F. Mouthereau, and O. Lacombe (2006), Lithospheric bulge in the West Taiwan Basin, *Basin Res.*, *18*, 277–299, doi:10.1111/j.1365-2117.2006.00296.x.

Theunissen, T., S. Lallemand, Y. Font, S. Gautier, C.-S. Lee, W.-T. Liang, F. Wu, and T. Berthet (2012), Crustal deformation at the southernmost part of the Ryukyu subduction (East Taiwan) as revealed by new marine seismic experiments, *Tectonophysics*, *578*, 10–30, doi:10.1016/j.tecto.2012.04.011.

Van Avendonk, H. J. A., A. J. Harding, J. A. Orcutt, and W. S. Holbrook (2001), Hybrid shortest path and ray bending method for traveltime and raypath calculations, *Geophysics*, *66*, 648–653.

Van Avendonk, H. J. A., W. S. Holbrook, D. Okaya, J. K. Austin, F. Davey, and T. Stern (2004a), Continental crust under compression: A seismic refraction study of SIGHT Transect I, South Island, New Zealand, *J. Geophys. Res.*, *109*, B06302, doi:10.1029/2003JB002790.

Van Avendonk, H. J. A., D. J. Shillington, W. S. Holbrook, and M. J. Hornbach (2004b), Inferring crustal structure in the Aleutian Arc from a sparse wide-angle seismic data set, *Geochem. Geophys. Geosyst.*, *5*, Q08008, doi:10.1029/2003GC000664.

White, R. S., D. McKenzie, and R. K. O'Nions (1992), Oceanic crustal thickness from seismic measurements and rare earth element inversions, *J. Geophys. Res.*, *97*, 19,683–19,715, doi:10.1029/92JB01749.

Willett, S. D., D. Fisher, C. Fuller, Y. En-Chao, and L. Chia-Yu (2003), Erosion rates and orogenic-wedge kinematics in Taiwan inferred from fission-track thermochronometry, *Geology*, *31*, 945–948, doi:10.10.1130/G19702.1.

Wu, F. T., C. S. Chang, and Y. M. Wu (2004), Precisely relocated hypocentres, focal mechanisms and active orogeny in Central Taiwan, in *Aspects of the Tectonic Evolution of China*, edited by J. Malpas et al., *Geol. Soc. Spec. Publ.*, *226*, 333–354, London.

Wu, Y.-M., C.-H. Chang, L. Zhao, J. B. H. Shyu, Y.-G. Chen, K. Sieh, and J.-P. Avouac (2007), Seismic tomography of Taiwan: Improved constraints from a dense network of strong motion stations, *J. Geophys. Res.*, *112*, B08312, doi:10.1029/2007JB004983.

Yamato, P., F. Mouthereau, and E. Burov (2009), Taiwan mountain building: Insights from 2-D thermomechanical modelling of a rheologically stratified lithosphere, *Geophys. J. Int.*, *176*, 307–326, doi:10.1111/j.1365-246X.2008.03977.x.

Yu, S.-B., and L.-C. Kuo (2001), Present-day crustal motion along the Longitudinal Valley Fault, eastern Taiwan, *Tectonophysics*, *333*, 199–217, doi:10.1016/S0040-1951(00)00275-4.

Yu, S.-B., L.-C. Kuo, R. S. Punongbayan, and E. G. Ramos (1999), GPS observation of crustal deformation in the Taiwan-Luzon region, *Geophys. Res. Lett.*, *26*, 923–926, doi:10.1029/1999GL900148.

Yue, L.-F., J. Suppe, and J.-H. Hung (2005), Structural geology of a classic thrust belt earthquake: The 1999 Chi-Chi earthquake Taiwan (MwZ7.6), *J. Struct. Geol.*, *27*, 2058–2083, doi:10.1016/j.jsg.2005.05.020.